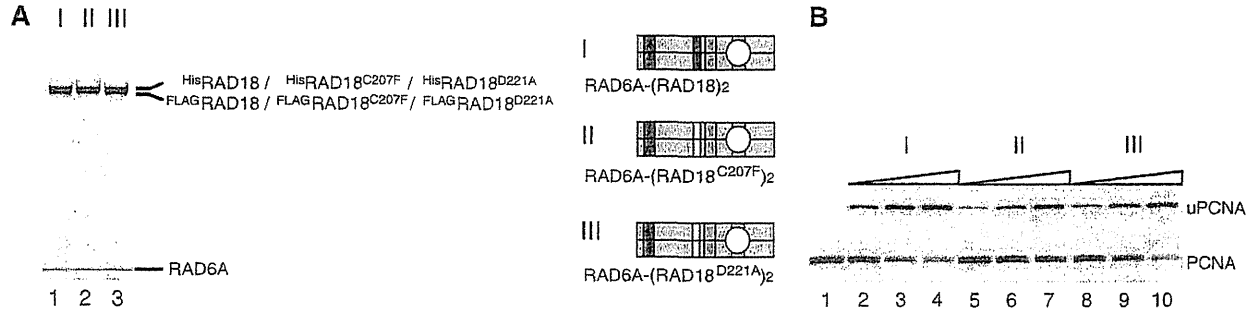

Figure 5. Analysis of ligase activity and complex formation with UBZ mutants of RAD18. (**A**) Purified complexes (3.7 pmol) were analyzed by SDS–PAGE followed by staining with CBB. I, RAD6A–(^{His}RAD18–^{FLAG}RAD18); II, RAD6A–(^{His}RAD18^{C207F}–^{FLAG}RAD18^{C207F}); III, RAD6A–(^{His}RAD18^{D221A}–^{FLAG}RAD18^{D221A}). Structures are represented schematically, UBZ domains with a mutation being shown in white boxes. (**B**) Ligase activity of the respective RAD6A–RAD18 complexes. Increasing amounts of the complexes (0.5, 1 and 2 pmol) shown in (A) were subjected to standard assays.

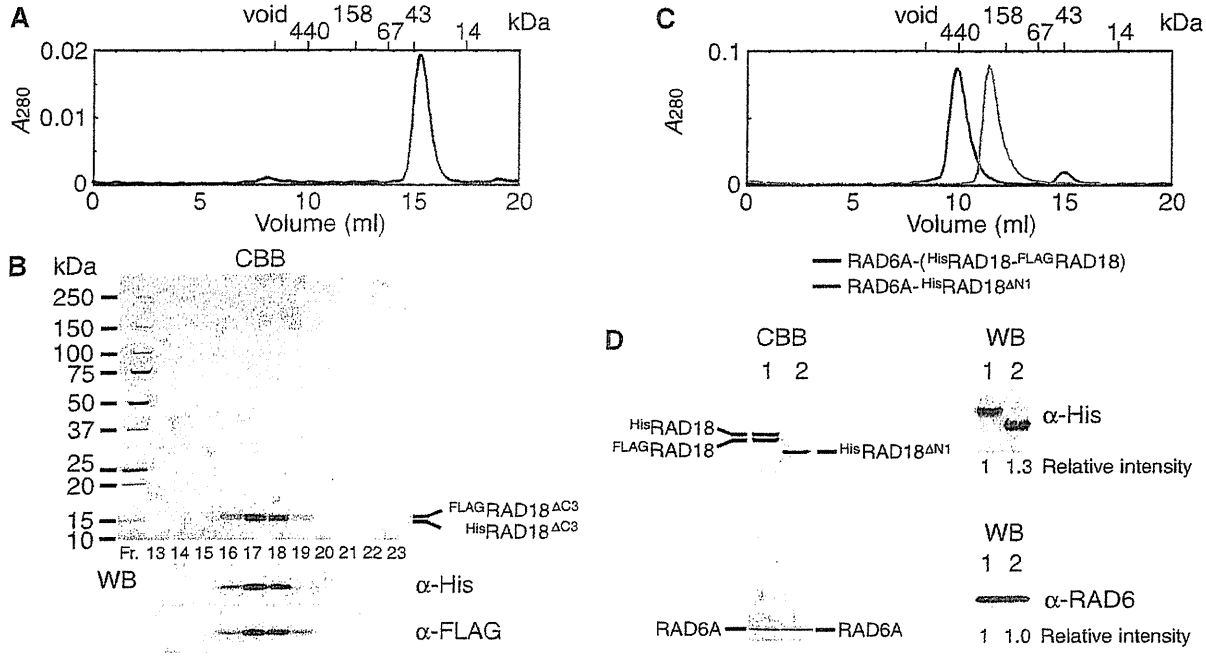

Figure 6. Analysis of RING domain for dimerization of RAD18. (**A**) Elution profile of ^{His}RAD18$^{\Delta C2}$–^{FLAG}RAD18$^{\Delta C2}$ complexes from a Superdex 200 gel filtration column. The size markers, ferritin (440 kDa), aldolase (158 kDa), albumin (67 kDa), ovalbumin (43 kDa) and ribonuclease A (14 kDa) were eluted in 10.09, 12.26, 13.74, 14.98 and 17.56 ml, respectively. The complex was eluted in 15.35 ml, estimated the apparent molecular mass of the complex to be 37 kDa from a standard curve of the marker proteins. (**B**) Analysis of fractions eluted from a Superdex 200 gel filtration column (A). Fractions between 13 and 18.5 ml were analyzed by SDS–PAGE followed by staining with CBB and western blotting probed with the indicated antibodies. ^{His}RAD18$^{\Delta C2}$ (15.1 kDa) migrated slightly faster than ^{FLAG}RAD18$^{\Delta C2}$ (14.2 kDa). (**C**) Elution profile of RAD6A–(^{His}RAD18–^{FLAG}RAD18) and RAD6A–^{His}RAD18$^{\Delta N1}$ complexes from a Superdex 200 gel filtration column. Respective complexes were eluted in 9.77 and 11.45 ml, corresponding to 490 and 220 kDa of the apparent molecular masses, and 62 and 52 Å of Stokes' radius, estimated from a standard curve of the marker proteins. (**D**) Peak fractions of gel filtration chromatography (C) were analyzed by SDS–PAGE followed by CBB staining and western blotting probed with the indicated antibodies. Relative chemiluminescence signals detected with a CCD camera are shown. Lane 1, RAD6A–(^{His}RAD18–^{FLAG}RAD18) (3.7 pmol as a trimer); lane 2, RAD6A–^{His}RAD18$^{\Delta N1}$ (3.7 pmol as a dimer).

as indicated in Figure 3A. We found that RING mutants with C25A, C25S, C25F, I27A, C28S, C27F or F53A/L54A substitutions eluted in void volumes on gel filtration chromatography, suggesting these mutants to form large aggregates due to highly disordered structures by misfolding. Therefore we did not further analyze them. However, we could successfully obtain one mutant complex containing I50A/R51A substitutions in RAD18 (hereafter designated as RAD18^{RING}, see Figures 3A and 7A, lane 2). A previous report suggested, based on the crystal structure of the c-Cbl-UbcH7 complex, that the amino acid residues Ile50 and Arg51 of RAD18 should be located in a predicted RAD6-interacting α-helix (2). Thus, it was expected that I50A/R51A mutations would affect

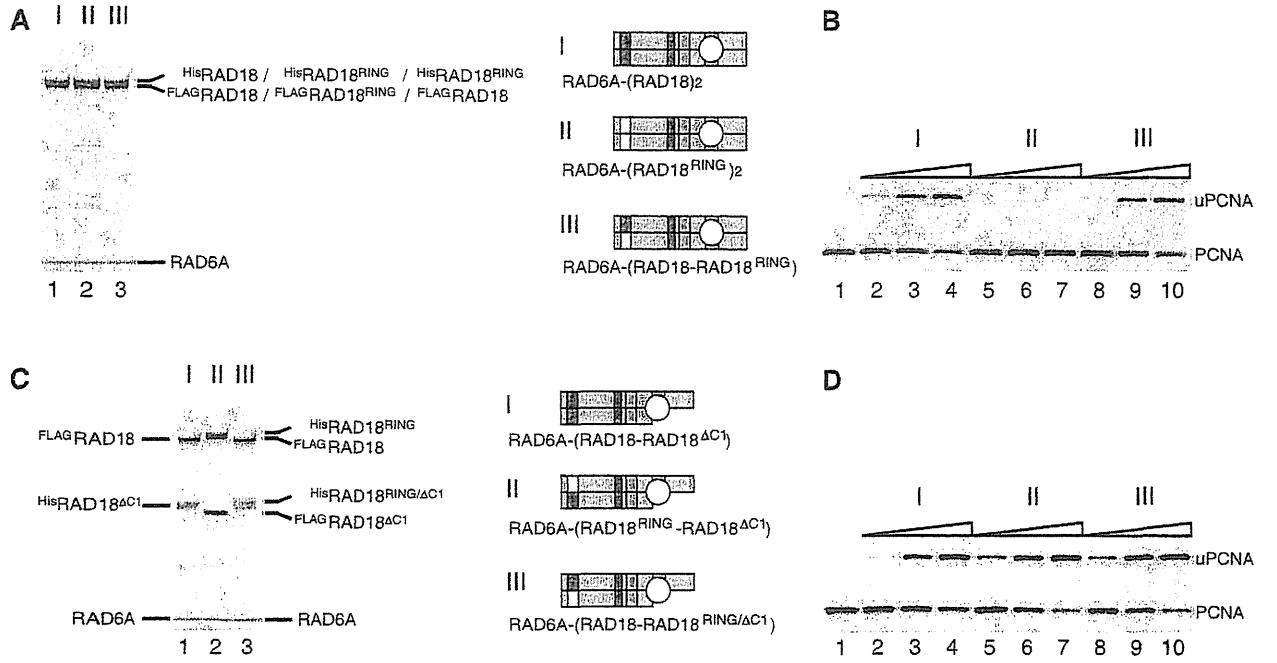

Figure 7. Analysis of ligase activity and complex formation of a RING mutant of RAD18. (**A**) Purified complexes (3.7 pmol) were analyzed by SDS–PAGE followed by staining with CBB. I, RAD6A–(^{His}RAD18–^{FLAG}RAD18); II, RAD6A–(^{His}RAD18^{RING}_^{FLAG}RAD18^{RING}); III, RAD6A–(^{His}RAD18^{RING}_^{FLAG}RAD18). Structures are represented schematically. RING domains with a mutation being shown in white boxes. (**B**) Ligase activities of the respective RAD6A–RAD18 complexes. Increasing amounts of the complexes (0.5, 1 and 2 pmol) shown in (A) were subjected to standard assays. (**C**) Purified complexes (3.7 pmol) were analyzed by SDS–PAGE followed by staining with CBB. I, RAD6A–(^{His}RAD18$^{\Delta C1}$_^{FLAG}RAD18); II, RAD6A–(^{His}RAD18^{RING}_^{FLAG}RAD18$^{\Delta C1}$); III, RAD6A–(^{His}RAD18$^{RING/\Delta C1}$_^{FLAG}RAD18). (**D**) Ligase activities of the respective RAD6A–RAD18 complexes. Increasing amounts of the complexes (0.5, 1 and 2 pmol) shown in (C) were subjected to standard assays.

the ligase activity of RAD18. In fact, it was much reduced when compared to that of the wild-type complex (Figure 7B). Then, we reconstituted a hetero complex with the mutant and wild-type, RAD6A–(^{His}RAD18^{RING}_^{FLAG}RAD18) (Figure 7A, lane 3). Surprisingly, its ligase activity was essentially identical to that of the wild-type (Figure 7B), indicating that an interaction between RAD6 and only one RING domain in the two RAD18 subunits is sufficient for ligase activity. In addition, I50A/R51A mutations were combined with the ΔC1 mutation and two mutant complexes, RAD6A–(^{His}RAD18^{RING}_^{FLAG}RAD18$^{\Delta C1}$) and RAD6A–(^{His}RAD18$^{RING/\Delta C1}$_^{FLAG}RAD18) were reconstituted (Figure 7C). Analysis of their ligase activities demonstrated these to be as active as the wild-type (Figure 7D), indicating that one RAD6 molecule in the complex has the potential to interact with either subunit of the RAD18 dimer.

Functional interaction between SAP and R6BD for ligase activity

It has been shown that the SAP domain of RAD18 has DNA-binding activity (15,38), which is separable from its essential function for ligase activity (38). When a mutant RAD18 containing L250A/L265A substitutions (hereafter designated as RAD18^{SAP}, see Figure 3D) was successfully reconstituted into the ternary complex, RAD6A–(^{His}RAD18^{SAP}_^{FLAG}RAD18^{SAP}) (Figure 8A, lane 2), the ligase activity of the mutant complex was reduced to an undetectable level (Figure 8B). However, activity was restored in a hetero complex with the wild-type, RAD6A–(^{His}RAD18^{SAP}_^{FLAG}RAD18) (Figure 8B), demonstrating that only one of the two SAP domains in the complex is sufficient for the essential SAP function. Next, the SAP mutation was combined with the ΔC1 mutation to reconstitute RAD6A–(^{His}RAD18^{SAP}_^{FLAG}RAD18$^{\Delta C1}$) and RAD6–(^{His}RAD18$^{SAP/\Delta C1}$_^{FLAG}RAD18) (Figure 8C). Interestingly, the former had quite reduced ligase activity, but the latter exhibited the wild-type level (Figure 8D), indicating that the active SAP domain should be present on the same RAD18 molecule to which RAD6 binds. In contrast, such functional interaction was not observed between RING and SAP mutants; ligase activities of RAD6A–(^{His}RAD18$^{RING/SAP}$_^{FLAG}RAD18) and RAD6–(^{His}RAD18^{RING}_^{FLAG}RAD18^{SAP}) complexes (Figure 8E) were similar to that of wild-type (Figure 8F).

DISCUSSION

In this study, we established a method to distinguish between the two subunits of RAD18 in the RAD6–(RAD18)$_2$ complex by introducing different tags at the N-termini. This enabled us to purify RAD18 complexes composed of wild–wild, wild–mutant or mutant–mutant subunits and facilitated analysis of structure–function relationships in RAD18.

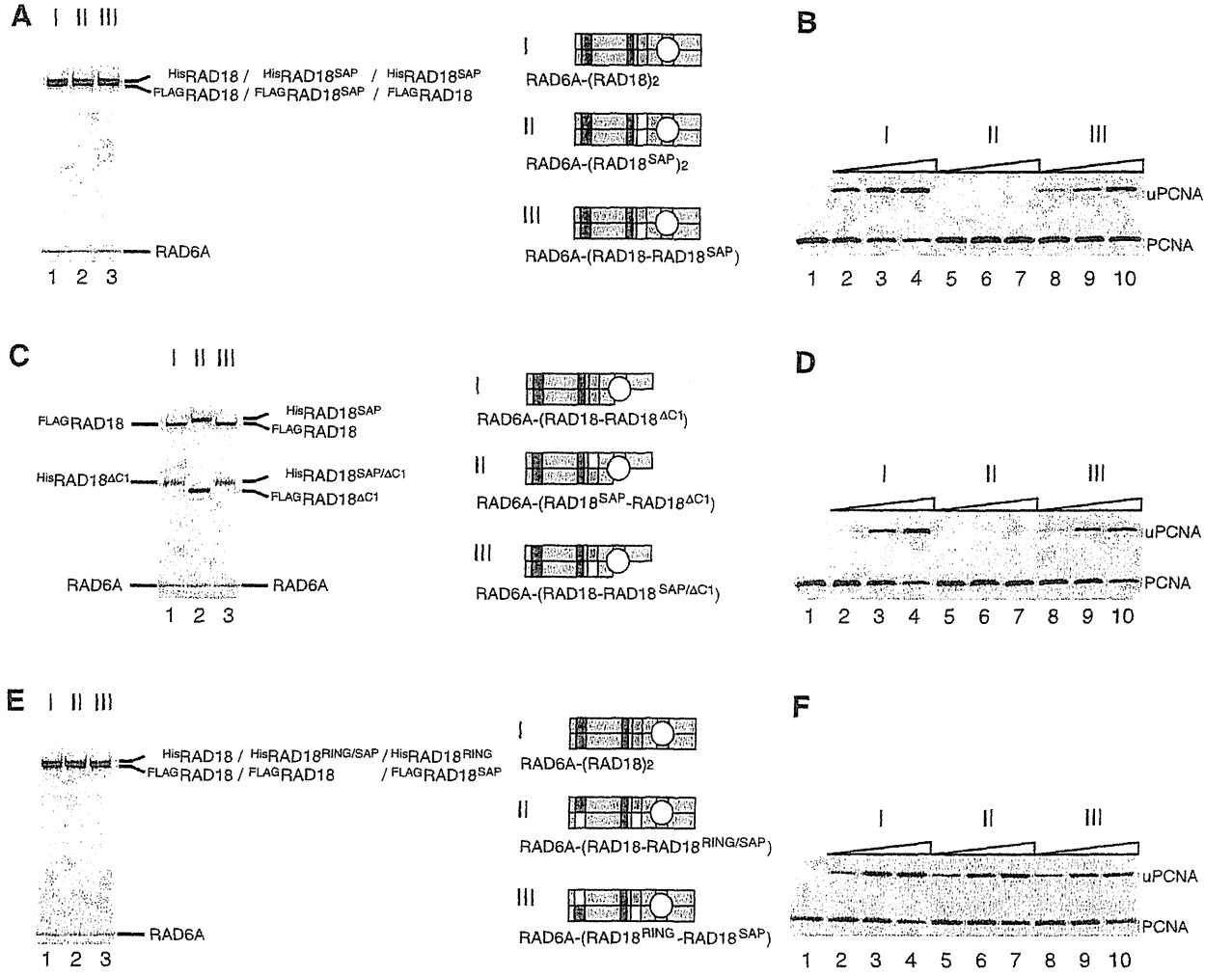

Figure 8. *Analysis of ligase activity and complex formation of a SAP mutant of RAD18.* (**A**) Purified complexes (3.7 pmol) were analyzed by SDS–PAGE followed by staining with CBB. I, RAD6A–(^{His}RAD18–^{FLAG}RAD18); II, RAD6A–(^{His}RAD18^{SAP}–^{FLAG}RAD18^{SAP}); III, RAD6A–(^{His}RAD18^{SAP}–^{FLAG}RAD18). Structures were represented schematically, SAP domains with a mutation being shown in white boxes. (**B**) Ligase activities of the respective RAD6A–RAD18 complexes. Increasing amounts of the complexes (0.5, 1 and 2 pmol) shown in (A) were subjected to standard assays. (**C**) Purified complexes (3.7 pmol) were analyzed by SDS–PAGE followed by staining with CBB. I, RAD6A–(^{His}RAD18$^{\Delta C1}$–^{FLAG}RAD18); II, RAD6A–(^{His}RAD18^{SAP}–^{FLAG}RAD18$^{\Delta C1}$); III, RAD6A–(^{His}RAD18$^{SAP/\Delta C1}$–^{FLAG}RAD18). (**D**) Ligase activities of the respective RAD6A–RAD18 complexes. Increasing amounts of the complexes (0.5, 1 and 2 pmol) shown in (C) were subjected to standard assays. (**E**) Purified complexes (3.7 pmol) were analyzed by SDS–PAGE followed by staining with CBB. I, RAD6A–(^{His}RAD18–^{FLAG}RAD18); II, RAD6A–(^{His}RAD18$^{RING/SAP}$–^{FLAG}RAD18); III, RAD6A–(^{His}RAD18^{RING}–^{FLAG}RAD18^{SAP}). (**F**) Ligase activities of the respective RAD6A–RAD18 complexes. Increasing amounts of the complexes (0.5, 1 and 2 pmol) shown in (E) were subjected to standard assays.

Previously, it was considered that the RAD6–RAD18 complex could be composed of two RAD6 and two RAD18, since the observations that RAD18 binds to RAD6 and it forms a dimer led to the assumption that each RAD18 molecule in the dimer should bind to RAD6 (15,20,21). However, there is little evidence for such an assignment based on the stoichiometry of RAD6. In this study, we provided hard lines of evidence that the complex is composed of one subunit of RAD6 and two subunits of RAD18, so that the overall structure of the ternary complex should be asymmetric.

The RING domains in E3s have an essential function in ligase activity by mediating interactions with E2s. Zheng *et al.* (2) have suggested, on the basis of the crystal structure of the c-Cbl-UbcH7 complex, that amino acid residues I50 and R51 in the RING domain of RAD18 are located in a predicted RAD6-interacting α-helix. Consistent with this, a mutant complex containing I50A/R51A substitutions in both RAD18 subunits exhibited severely reduced ligase activity, probably due to an impaired interaction between the altered RING domain and RAD6A. When the mutant subunit was complexed with wild-type RAD18 subunit, ligase activity was restored to the wild-type level, indicating that only one of the two RING domains is necessary for enzyme function. Furthermore, even when the RING mutation

was combined with a deletion mutation of R6BD in the same or other RAD18 subunit, the complexes exhibited robust ligase activity. These results imply that RAD6 can bind in either one of the two R6BDs, then interacting with one of the two RING domains in the RAD18 dimer.

Why should the RING domain of RAD18 form a dimer? We found that inactivation of one RING domain does not affect the ligase activity, indicating that the close proximity of two active RING domains in RAD18 is not important for the enzyme function. From our observations that some RING mutants such as C25A, C25S, C25F, I27A, C28S, C28F and F53A/L54A, probably disrupting the RING structure (Figure 3D), appeared to form large aggregates, we suggest that the RING structure is required for stable dimerization, which is in turn necessary for sustaining the functionally active RING structure of RAD18. From the results, we cannot exclude the possibility of retention of some enzyme functions even in aggregates. Indeed, it has been reported that the C28F mutant can fully complement the homologous recombination defects of RAD18-null cells (39).

The SAP domain is a unique eukaryotic module involved in sequence- or structure-specific DNA binding (36,38,49–52). Additionally, in RAD18 it has an essential role in ligase activity, separable from its function in DNA binding (38). We further demonstrated that one of the two SAP domains in the RAD6–$(RAD18)_2$ complex is sufficient for ligase activity. Interestingly, experiments using hetero complexes, in which mutation in the SAP domain was combined with a deletion mutation of R6BD, revealed an interesting relationship between SAP and R6BD. Although one of the two SAP domains and one of the two R6BDs are sufficient for enzyme activity, the active SAP domain should be present on the same RAD18 molecule to which RAD6 binds in the complex. It makes a sharp contrast to the case of RING mutant as described above. A simple explanation is that the SAP domain acts as a hinge connecting the R6BD and RING domain to enable precise juxtaposition between RING and RAD6. This might be very important for ligase activity because a deletion mutant of R6BD hardly supported PCNA ubiquitination in the presence of an excess amount of RAD6A, which should be high enough to detect ligase activities for many other E2–E3 pairs (4–6,9–2). It seems likely that binding affinity between RAD6 and the RING domain of RAD18 is very low. That could be the reason why R6BD is essential for ligase activity of the RAD6–RAD18 complex. The tight interaction between RAD6 and R6BD confers on the complex the ability to monoubiquitinate PCNA, also inhibiting the activity of RAD6 catalyzing ubiquitin chain formation (19).

In the above, we have shown that RAD6 and RAD18 forms a ternary complex, RAD6–$(RAD18)_2$ and demonstrated that one R6BD site is sufficient for the ligase activity. Then, a question that immediately arises is why RAD6 can bind to one of the two R6BD sites, but not to both of them. Although we have no experimental data to answer the question at the moment, such a case is not unprecedented. CHIP (*C*-terminal of *H*sp70 *i*nteracting *p*rotein), a protein containing a C-terminal Ubox domain (similar to RING) and an N-terminal TPR domain, forms an asymmetric dimer mediated by the Ubox domains, in which only one of the two Ubox domains is available for binding to E2 (Ubc13) because the other Ubox domain is blocked due to interaction with the TPR domain (53). It is tempting to speculate that a segment including R6BD located in a C-terminal portion of the two RAD18 subunits may interact with one of the two RING domains, consequently preventing the R6BD from interacting with RAD6. Thus, one RAD6 molecule can bind to the other R6BD and is positioned closely to another unoccupied RING domain for catalyzing the ligase function. Evidently, further experiments are required to elucidate this interesting possibility.

During the course of finally completing this manuscript, we have learned that Huang and co-workers have recently determined the structure of a RAD18 RING(1–99) dimer, also showing that this binds to RAD6 at a 2:2 ratio, whereas the full-length RAD18 dimer binds only to a single RAD6 molecule (54). Our study was conducted independently of their work.

SUPPLEMENTARY DATA

Supplementary Data are available at NAR Online: Supplementary Materials and Methods, Supplementary References [26,45,55].

ACKNOWLEDGEMENTS

The authors thank Dr Toshiki Tsurimoto (Kyushu University, Fukuoka, Japan) and Dr Tomohiko Ohta (St Marianna University School of Medicine, Kanagawa, Japan) for providing PCNA expression and ubiquitin-encoding plasmids, respectively. The authors would also like to express our appreciation to Dr Haruo Ohmori (Kyoto University, Kyoto, Japan) for his critical reading of manuscripts and valuable suggestions. The authors are grateful to Fumie Okubo, Kazumi Shimamoto and Mai Yoshida for their laboratory assistance.

FUNDING

Grants-in-Aid from the Ministry of Education, Culture, Sports, Science and Technology of Japan (to Y.M. and K.K.); Grants-in-Aid for Cancer Research from the Ministry of Health, Labour and Welfare (to K.K.). Funding for open access charge: Grants-in-Aid from the Ministry of Education, Culture, Sports, Science and Technology of Japan.

Conflict of interest statement. None declared.

REFERENCES

1. Deshaies,R.J. and Joazeiro,C.A. (2009) RING domain E3 ubiquitin ligases. *Annu. Rev. Biochem.*, **78**, 399–434.
2. Zheng,N., Wang,P., Jeffrey,P.D. and Pavletich,N.P. (2000) Structure of a c-Cbl-UbcH7 complex: RING domain function in ubiquitin-protein ligases. *Cell*, **102**, 533–539.

3. Brzovic,P.S., Rajagopal,P., Hoyt,D.W., King,M.C. and Klevit,R.E. (2001) Structure of a BRCA1-BARD1 heterodimeric RING-RING complex. *Nat. Struct. Biol.*, **8**, 833–837.
4. Hashizume,R., Fukuda,M., Maeda,I., Nishikawa,H., Oyake,D., Yabuki,Y., Ogata,H. and Ohta,T. (2001) The RING heterodimer BRCA1-BARD1 is a ubiquitin ligase inactivated by a breast cancer-derived mutation. *J. Biol. Chem.*, **276**, 14537–14540.
5. Xia,Y., Pao,G.M., Chen,H.W., Verma,I.M. and Hunter,T. (2003) Enhancement of BRCA1 E3 ubiquitin ligase activity through direct interaction with the BARD1 protein. *J. Biol. Chem.*, **278**, 5255–5263.
6. Buchwald,G., van der Stoop,P., Weichenrieder,O., Perrakis,A., van Lohuizen,M. and Sixma,T.K. (2006) Structure and E3-ligase activity of the Ring-Ring complex of polycomb proteins Bmi1 and Ring1b. *EMBO J.*, **25**, 2465–2474.
7. Satijn,D.P. and Otte,A.P. (1999) RING1 interacts with multiple Polycomb-group proteins and displays tumorigenic activity. *Mol. Cell. Biol.*, **19**, 57–68.
8. Kawai,H., Lopez-Pajares,V., Kim,M.M., Wiederschain,D. and Yuan,Z.M. (2007) RING domain-mediated interaction is a requirement for MDM2's E3 ligase activity. *Cancer Res.*, **67**, 6026–6030.
9. Linares,L.K., Hengstermann,A., Ciechanover,A., Muller,S. and Scheffner,M. (2003) HdmX stimulates Hdm2-mediated ubiquitination and degradation of p53. *Proc. Natl Acad. Sci. USA*, **100**, 12009–12014.
10. Linke,K., Mace,P.D., Smith,C.A., Vaux,D.L., Silke,J. and Day,C.L. (2008) Structure of the MDM2/MDMX RING domain heterodimer reveals dimerization is required for their ubiquitylation in trans. *Cell Death Differ.*, **15**, 841–848.
11. Mace,P.D., Linke,K., Feltham,R., Schumacher,F.R., Smith,C.A., Vaux,D.L., Silke,J. and Day,C.L. (2008) Structures of the cIAP2 RING domain reveal conformational changes associated with ubiquitin-conjugating enzyme (E2) recruitment. *J. Biol. Chem.*, **283**, 31633–31640.
12. Liew,C.W., Sun,H., Hunter,T. and Day,C.L. (2010) RING domain dimerization is essential for RNF4 function. *Biochem. J.*, **431**, 23–29.
13. Bailly,V., Lamb,J., Sung,P., Prakash,S. and Prakash,L. (1994) Specific complex formation between yeast RAD6 and RAD18 proteins: a potential mechanism for targeting RAD6 ubiquitin-conjugating activity to DNA damage sites. *Genes Dev.*, **8**, 811–820.
14. Bailly,V., Lauder,S., Prakash,S. and Prakash,L. (1997) Yeast DNA repair proteins Rad6 and Rad18 form a heterodimer that has ubiquitin conjugating, DNA binding, and ATP hydrolytic activities. *J. Biol. Chem.*, **272**, 23360–23365.
15. Notenboom,V., Hibbert,R.G., van Rossum-Fikkert,S.E., Olsen,J.V., Mann,M. and Sixma,T.K. (2007) Functional characterization of Rad18 domains for Rad6, ubiquitin, DNA binding and PCNA modification. *Nucleic Acids Res.*, **35**, 5819–5830.
16. Bailly,V., Prakash,S. and Prakash,L. (1997) Domains required for dimerization of yeast Rad6 ubiquitin-conjugating enzyme and Rad18 DNA binding protein. *Mol. Cell. Biol.*, **17**, 4536–4543.
17. Watanabe,K., Tateishi,S., Kawasuji,M., Tsurimoto,T., Inoue,H. and Yamaizumi,M. (2004) Rad18 guides polη to replication stalling sites through physical interaction and PCNA monoubiquitination. *EMBO J.*, **23**, 3886–3896.
18. Tateishi,S., Sakuraba,Y., Masuyama,S., Inoue,H. and Yamaizumi,M. (2000) Dysfunction of human Rad18 results in defective postreplication repair and hypersensitivity to multiple mutagens. *Proc. Natl Acad. Sci. USA*, **97**, 7927–7932.
19. Hibbert,R.G., Huang,A., Boelens,R. and Sixma,T.K. (2011) E3 ligase Rad18 promotes monoubiquitination rather than ubiquitin chain formation by E2 enzyme Rad6. *Proc. Natl Acad. Sci. USA*, **108**, 5590–5595.
20. Miyase,S., Tateishi,S., Watanabe,K., Tomita,K., Suzuki,K., Inoue,H. and Yamaizumi,M. (2005) Differential regulation of Rad18 through Rad6-dependent mono- and polyubiquitination. *J. Biol. Chem.*, **280**, 515–524.
21. Ulrich,H.D. and Jentsch,S. (2000) Two RING finger proteins mediate cooperation between ubiquitin-conjugating enzymes in DNA repair. *EMBO J.*, **19**, 3388–3397.
22. Friedberg,E.C., Walker,G.C., Siede,W., Wood,R.D., Schultz,R.A. and Ellenberger,T. (2006) DNA repair and mutagenesis. *2nd edn.* ASM, Washington, DC.
23. Hoege,C., Pfander,B., Moldovan,G.L., Pyrowolakis,G. and Jentsch,S. (2002) RAD6-dependent DNA repair is linked to modification of PCNA by ubiquitin and SUMO. *Nature*, **419**, 135–141.
24. Garg,P. and Burgers,P.M. (2005) Ubiquitinated proliferating cell nuclear antigen activates translesion DNA polymerases η and REV1. *Proc. Natl Acad. Sci. USA*, **102**, 18361–18366.
25. Haracska,L., Unk,I., Prakash,L. and Prakash,S. (2006) Ubiquitylation of yeast proliferating cell nuclear antigen and its implications for translesion DNA synthesis. *Proc. Natl Acad. Sci. USA*, **103**, 6477–6482.
26. Masuda,Y., Piao,J. and Kamiya,K. (2010) DNA replication-coupled PCNA mono-ubiquitination and polymerase switching in a human *in vitro* system. *J. Mol. Biol.*, **396**, 487–500.
27. Unk,I., Hajdu,I., Fatyol,K., Hurwitz,J., Yoon,J.H., Prakash,L., Prakash,S. and Haracska,L. (2008) Human HLTF functions as a ubiquitin ligase for proliferating cell nuclear antigen polyubiquitination. *Proc. Natl Acad. Sci. USA*, **105**, 3768–3773.
28. Unk,I., Hajdu,I., Fatyol,K., Szakal,B., Blastyak,A., Bermudez,V., Hurwitz,J., Prakash,L., Prakash,S. and Haracska,L. (2006) Human SHPRH is a ubiquitin ligase for Mms2-Ubc13-dependent polyubiquitylation of proliferating cell nuclear antigen. *Proc. Natl Acad. Sci. USA*, **103**, 18107–18112.
29. Bienko,M., Green,C.M., Crosetto,N., Rudolf,F., Zapart,G., Coull,B., Kannouche,P., Wider,G., Peter,M., Lehmann,A.R. *et al.* (2005) Ubiquitin-binding domains in Y-family polymerases regulate translesion synthesis. *Science*, **310**, 1821–1824.
30. Wood,A., Garg,P. and Burgers,P.M. (2007) A ubiquitin-binding motif in the translesion DNA polymerase Rev1 mediates its essential functional interaction with ubiquitinated proliferating cell nuclear antigen in response to DNA damage. *J. Biol. Chem.*, **282**, 20256–20263.
31. Zhuang,Z., Johnson,R.E., Haracska,L., Prakash,L., Prakash,S. and Benkovic,S.J. (2008) Regulation of polymerase exchange between Polη and Polδ by monoubiquitination of PCNA and the movement of DNA polymerase holoenzyme. *Proc. Natl Acad. Sci. USA*, **105**, 5361–5366.
32. Day,T.A., Palle,K., Barkley,L.R., Kakusho,N., Zou,Y., Tateishi,S., Verreault,A., Masai,H. and Vaziri,C. (2010) Phosphorylated Rad 18 directs DNA polymerase η to sites of stalled replication. *J. Cell. Biol.*, **191**, 953–966.
33. Bish,R.A. and Myers,M.P. (2007) Werner helicase-interacting protein 1 binds polyubiquitin via its zinc finger domain. *J. Biol. Chem.*, **282**, 23184–23193.
34. Crosetto,N., Bienko,M., Hibbert,R.G., Perica,T., Ambrogio,C., Kensche,T., Hofmann,K., Sixma,T.K. and Dikic,I. (2008) Human Wrnip1 is localized in replication factories in a ubiquitin-binding zinc finger-dependent manner. *J. Biol. Chem.*, **283**, 35173–35185.
35. Hofmann,K. (2009) Ubiquitin-binding domains and their role in the DNA damage response. *DNA Repair*, **8**, 544–556.
36. Aravind,L. and Koonin,E.V. (2000) SAP - a putative DNA-binding motif involved in chromosomal organization. *Trends Biochem. Sci.*, **25**, 112–114.
37. Nakajima,S., Lan,L., Kanno,S., Usami,N., Kobayashi,K., Mori,M., Shiomi,T. and Yasui,A. (2006) Replication-dependent and -independent responses of RAD18 to DNA damage in human cells. *J. Biol. Chem.*, **281**, 34687–34695.
38. Tsuji,Y., Watanabe,K., Araki,K., Shinohara,M., Yamagata,Y., Tsurimoto,T., Hanaoka,F., Yamamura,K., Yamaizumi,M. and Tateishi,S. (2008) Recognition of forked and single-stranded DNA structures by human RAD18 complexed with RAD6B protein triggers its recruitment to stalled replication forks. *Genes Cells*, **13**, 343–354.
39. Huang,J., Huen,M.S., Kim,H., Leung,C.C., Glover,J.N., Yu,X. and Chen,J. (2009) RAD18 transmits DNA damage signalling to elicit homologous recombination repair. *Nat. Cell. Biol.*, **11**, 592–603.
40. Fukuda,K., Morioka,H., Imajou,S., Ikeda,S., Ohtsuka,E. and Tsurimoto,T. (1995) Structure-function relationship of the eukaryotic DNA replication factor, proliferating cell nuclear antigen. *J. Biol. Chem.*, **270**, 22527–22534.

41. Masuda,Y., Suzuki,M., Piao,J., Gu,Y., Tsurimoto,T. and Kamiya,K. (2007) Dynamics of human replication factors in the elongation phase of DNA replication. *Nucleic Acids Res.*, **35**, 6904–6916.
42. Tomida,J., Masuda,Y., Hiroaki,H., Ishikawa,T., Song,I., Tsurimoto,T., Tateishi,S., Shiomi,T., Kamei,Y., Kim,J. *et al.* (2008) DNA damage-induced ubiquitylation of RFC2 subunit of replication factor C complex. *J. Biol. Chem.*, **283**, 9071–9079.
43. Niwa,H., Yamamura,K. and Miyazaki,J. (1991) Efficient selection for high-expression transfectants with a novel eukaryotic vector. *Gene*, **108**, 193–199.
44. Maki,H. and Kornberg,A. (1987) Proofreading by DNA polymerase III of *Escherichia coli* depends on cooperative interaction of the polymerase and exonuclease subunits. *Proc. Natl Acad. Sci. USA*, **84**, 4389–4392.
45. Studier,F.W., Rosenberg,A.H., Dunn,J.J. and Dubendorff,J.W. (1990) Use of T7 RNA polymerase to direct expression of cloned genes. *Methods Enzymol.*, **185**, 60–89.
46. Siegel,L.M. and Monty,K.J. (1966) Determination of molecular weights and frictional ratios of proteins in impure systems by use of gel filtration and density gradient centrifugation. Application to crude preparations of sulfite and hydroxylamine reductases. *Biochim. Biophys. Acta*, **112**, 346–362.
47. Worthylake,D.K., Prakash,S., Prakash,L. and Hill,C.P. (1998) Crystal structure of the *Saccharomyces cerevisiae* ubiquitin-conjugating enzyme Rad6 at 2.6 Å resolution. *J. Biol. Chem.*, **273**, 6271–6276.
48. Yuasa,M.S., Masutani,C., Hirano,A., Cohn,M.A., Yamaizumi,M., Nakatani,Y. and Hanaoka,F. (2006) A human DNA polymerase η complex containing Rad18, Rad6 and Rev1; proteomic analysis and targeting of the complex to the chromatin-bound fraction of cells undergoing replication fork arrest. *Genes Cells*, **11**, 731–744.
49. Ahn,J.S. and Whitby,M.C. (2003) The role of the SAP motif in promoting Holliday junction binding and resolution by SpCCE1. *J. Biol. Chem.*, **278**, 29121–29129.
50. Chou,C.H., Wang,J., Knuth,M.W. and Reeves,W.H. (1992) Role of a major autoepitope in forming the DNA binding site of the p70 (Ku) antigen. *J. Exp. Med.*, **175**, 1677–1684.
51. Gohring,F., Schwab,B.L., Nicotera,P., Leist,M. and Fackelmayer,F.O. (1997) The novel SAR-binding domain of scaffold attachment factor A (SAF-A) is a target in apoptotic nuclear breakdown. *EMBO J.*, **16**, 7361–7371.
52. Kipp,M., Gohring,F., Ostendorp,T., van Drunen,C.M., van Driel,R., Przybylski,M. and Fackelmayer,F.O. (2000) SAF-Box, a conserved protein domain that specifically recognizes scaffold attachment region DNA. *Mol. Cell. Biol.*, **20**, 7480–7489.
53. Zhang,M., Windheim,M., Roe,S.M., Peggie,M., Cohen,P., Prodromou,C. and Pearl,L.H. (2005) Chaperoned ubiquitylation–crystal structures of the CHIP U box E3 ubiquitin ligase and a CHIP-Ubc13-Uev1a complex. *Mol. Cell*, **20**, 525–538.
54. Huang,A., Hibbert,R.G., de Jong,R.N., Das,D., Sixma,T.K. and Boelens,R. (2011) Symmetry and asymmetry of the RING-RING dimer of Rad18. *J. Mol. Biol.*, **410**, 424–435.
55. Gomes,X.V., Gary,S.L. and Burgers,P.M. (2000) Overproduction in Escherichia coli and characterization of yeast replication factor C lacking the ligase homology domain. *J. Biol. Chem.*, **275**, 14541–14549.

10394–10407 *Nucleic Acids Research, 2012, Vol. 40, No. 20* *Published online 16 August 2012*
doi:10.1093/nar/gks763

En bloc transfer of polyubiquitin chains to PCNA *in vitro* is mediated by two different human E2–E3 pairs

Yuji Masuda[1,2,*], Miki Suzuki[2], Hidehiko Kawai[3], Asami Hishiki[4], Hiroshi Hashimoto[4], Chikahide Masutani[1], Takashi Hishida[5], Fumio Suzuki[3] and Kenji Kamiya[2,*]

[1]Department of Genome Dynamics, Research Institute of Environmental Medicine, Nagoya University, Furo-cho, Chikusa-ku, Nagoya 464-8601, [2]Department of Experimental Oncology, [3]Department of Molecular Radiobiology, Research Institute for Radiation Biology and Medicine, Hiroshima University, 1-2-3 Kasumi, Minami-ku, Hiroshima 734-8553, [4]Graduate School of Nanobioscience, Yokohama City University, 1-7-29 Suehiro-cho, Tsurumi-ku, Yokohama 230-0045 and [5]Department of Molecular Genetics, Graduate School of Life Sciences, Gakushuin University, 1-5-1 Mejiro, Toshima-ku, Tokyo 171-8588, Japan

Received April 24, 2012; Revised July 5, 2012; Accepted July 18, 2012

ABSTRACT

Post-replication DNA repair in eukaryotes is regulated by ubiquitination of proliferating cell nuclear antigen (PCNA). Monoubiquitination catalyzed by RAD6–RAD18 (an E2–E3 complex) stimulates translesion DNA synthesis, whereas polyubiquitination, promoted by additional factors such as MMS2–UBC13 (a UEV–E2 complex) and HLTF (an E3 ligase), leads to template switching in humans. Here, using an *in vitro* ubiquitination reaction system reconstituted with purified human proteins, we demonstrated that PCNA is polyubiquitinated predominantly via *en bloc* transfer of a pre-formed ubiquitin (Ub) chain rather than by extension of the Ub chain on monoubiquitinated PCNA. Our results support a model in which HLTF forms a thiol-linked Ub chain on UBC13 (UBC13~Ub_n) and then transfers the chain to RAD6~Ub, forming RAD6~Ub_{n+1}. The resultant Ub chain is subsequently transferred to PCNA by RAD18. Thus, template switching may be promoted under certain circumstances in which both RAD18 and HLTF are coordinately recruited to sites of stalled replication.

INTRODUCTION

DNA is continuously injured by environmental insult as well as endogenous metabolic products. Such DNA damage, unless removed by multiple mechanisms for excision repair, inhibits replicative DNA polymerase action during DNA replication (1). Post-replication repair, to restart DNA replication stalled at DNA damaged sites, features two sub-pathways, translesion DNA synthesis (TLS) and template switching (TS), which are regulated by mono- and polyubiquitination of proliferating cell nuclear antigen (PCNA) at Lys164, respectively (2). RAD6 (an E2 ubiquitin-conjugating enzyme) and RAD18 (an E3 ubiquitin ligase) together catalyze the monoubiquitination of PCNA (2–4). The resultant monoubiquitinated PCNA (monoUb-PCNA) then activates the TLS pathway, in which stalled replication proceeds beyond the damage site with the help of specialized TLS polymerases. MonoUb-PCNA is believed to stimulate the entry of TLS polymerases at stalled 3′-ends, and this activity is dependent on interactions between the ubiquitin (Ub) moiety of monoUb-PCNA and the Ub-binding domains of the TLS polymerases (5–9). However, TLS is a mutagenic process due to the utilization of damaged templates by low-fidelity TLS polymerases (1).

Polyubiquitination of PCNA requires a different E2–E3 pair, MMS2–UBC13, a stable complex of an ubiquitin E2 variant (UEV) and an E2, and RAD5 in yeast (hereafter referred to as yRAD5) (2) or in humans, the two RAD5 homologs, HLTF and SHPRH, which serve as the E3 ligase (10–14). MMS2–UBC13 complexes mediate the formation of ubiquitin chains with Lys63 linkages (15). Polyubiquitinated PCNA (polyUb-PCNA) promotes the TS pathway, in which the primer end stalled at the

*To whom correspondence should be addressed. Tel: +81 52 789 3871; Fax: +81 52 789 3890; Email: masuda@riem.nagoya-u.ac.jp
Correspondence may also be addressed to Kenji Kamiya. Tel: +81 82 257 5842; Fax: +81 82 257 5844; Email: kkamiya@hiroshima-u.ac.jp

The authors wish it to be known that, in their opinion, the first two authors should be regarded as joint First Authors.

damaged site is released from the damaged template and anneals with the newly synthesized daughter strand of the sister chromosome. The molecular mechanism(s) of TS are currently unknown, but it is believed that a complex set of biochemical reactions is involved. When the sophisticated TS reactions are successfully performed, this process is essentially error-free, as it utilizes a non-damaged template (1).

It has been argued, mainly on the basis of genetic data from yeast studies, that polyubiquitination of PCNA is downstream of monoubiquitination. Both mono- and polyubiquitination are dependent on yRAD6 and yRAD18; deletion or mutation of either one of these two proteins blocks both the TS and TLS pathways. By contrast, inactivation or deletion of yMMS2, yUBC13 or yRAD5 abolishes polyubiquitination of PCNA, but not monoubiquitination of PCNA, and thus blocks only the TS pathway (1,2). These data are consistent with results previously obtained from *in vitro* biochemical studies using purified yeast enzymes (16,17). The yRAD6–yRAD18 complex can monoubiquitinate PCNA at Lys164, whereas yMMS2–yUBC13 and yRAD5 are able to polyubiquitinate PCNA only in the presence of yRAD6–yRAD18 (16). There is general agreement that the ligase activity of yRAD5 mediates sequential transfer of Ub from yUBC13~Ub to monoUb-PCNA (16,17). An unresolved issue, however, is why the error-free TS pathway would require the formation of monoUb-PCNA as an intermediate, which could potentially promote the error-prone TLS pathway and interfere with the preservation of genetic information.

In the current study, we investigated the mechanism of PCNA polyubiquitination using an *in vitro* ubiquitination reaction system reconstituted with purified recombinant human proteins, including HLTF. The results point to the existence of a novel reaction mechanism for the polyubiquitination of PCNA via *en bloc* Ub chain transfer. Importantly, the reaction mechanism appears to be more efficient than the conventional mechanism of sequential addition of Ub monomers to the distal end of an Ub chain on PCNA. We discuss the implications of these *in vitro* findings in terms of the choice of pathway, TS or TLS, proceeding from stalled replication sites following DNA damage.

MATERIALS AND METHODS

Plasmids

Expression plasmids for PCNA, RFC, E1, RAD6A, the RAD6A–RAD18 complex and Ub have been described previously (7,18–21). Expression plasmids for MMS2 and UBC13 were constructed using the pET20 parental vector. For the production of MMS2–UBC13 complexes, *MMS2* and *UBC13* were co-expressed as a single operon under the control of the T7 promoter. *HLTF* was cloned into pBAD22A (obtained from National BioResource Project, National Institute of Genetics, Mishima, Japan), and expression was induced by arabinose. For the histidine-tagged proteins, the tag sequence of pET15 was ligated to the 5′-end of the start codons of the respective genes. For $^{His}USP2^{(258-605)}$, a truncated sequence corresponding to amino acids 258–605 was subcloned into pET15. Synthetic genes encoding the $^{His}PCNA–Ub^{GG}$ fusion proteins were constructed in pET28a.

Proteins

Isopeptidase T was purchased from Boston Biochem (E-322). Other recombinant human proteins were expressed in *Escherichia coli* strain BL21 (DE3) at 15°C and then purified by chromatography at 4°C using the indicated columns (GE Healthcare), unless otherwise indicated. PCNA, RFC, E1, RAD6A, RAD6A–RAD18 complexes and Ub were purified as described previously (7,18,19,21). MMS2–UBC13 complexes were purified by sequential chromatography on HiPrep DEAE FF, HiTrap SP XL, HiTrap SP HP, HiTrap Heparin HP and Superdex 200 columns. MMS2–$UBC13^{C87A}$ complexes were purified on HiTrap Heparin HP, HiTrap SP XL and HiTrap SP HP columns, and MMS2–^{FLAG}UBC13 complexes were purified on HiTrap Q FF, HiTrap SP HP and HiTrap Heparin HP columns. UBC13 was purified on HiPrep DEAE FF, HiTrap SP FF, HiTrap SP HP, HiTrap Heparin HP and Superdex 200 columns. HLTF was purified on HiTrap Heparin HP, HiTrap SP HP, HiTrap Q HP, HiTrap SP XL, Econopack CHT-II (BIO-RAD) and Superdex 200 columns. RAD6A–^{His}RAD18, ^{His}HLTF and the corresponding mutants of each were partially purified using HiTrap Chelating HP and Superdex 200 columns. $^{His}PCNA$, $^{His}PCNA–Ub^{K63R/\Delta GG}$ and $^{His}PCNA^{K164R}–Ub^{\Delta GG}$ were purified using HiTrap Chelating HP, HiTrap Q FF and Superdex 200 columns. $^{His}USP2^{(258-605)}$ was purified using HiTrap Chelating HP and Superdex 200 columns. MonoUb-PCNA was purified from *E. coli* overexpressing PCNA, E1 and RAD6A–RAD18, and ^{His}Ub. ^{His}yRAD5 was overexpressed in strain BL21 Star (DE3) (Life Technologies), which harbors pMStRNA1 (22), and partially purified using a HiTrap Chelating HP column.

Ubiquitination assays

The standard reaction mixture (25 µl) contained 20 mM HEPES–NaOH (pH 7.5), 50 mM NaCl, 0.2 mg/ml BSA, 1 mM DTT, 10 mM $MgCl_2$, 1 mM ATP, poly(dA)-oligo(dT) (GE Healthcare) (100 ng) as the source of multiple primed single-stranded (mpss) DNA, PCNA (1.0 pmol trimer), RFC (0.70 pmol), E1 (0.85 pmol), RAD6A–RAD18 complexes (0.54 pmol trimer), MMS2–UBC13 complexes (16.4 pmol dimer), HLTF (1.3 pmol) and Ub (174 pmol). For the competition assays containing 1740 pmol Ub, 6 pmol E1 was introduced to overcome the inhibitory effect of large amounts of Ub (23,24). Reaction mixtures were prepared on ice and then incubated at 30°C for 10 min unless otherwise indicated. Reaction products were analyzed by immunoblot. Where indicated by 'reducing' or unless otherwise indicated, the samples were treated with sodium dodecyl sulphate (SDS) sample buffer containing 280 mM β-mercaptoethanol. Samples that were not treated with reducing agent were referred to as 'non-reducing'. Anti-PCNA (Santa Cruz, sc-7907), anti-UBC13 (IMGENEX, IMG-5634), anti-RAD6

(Abcam, ab31917), anti-Ub (Sigma, U5379) and anti-FLAG M2 monoclonal antibodies (Sigma, F 3165) were used as indicated. Immunoreactive proteins were visualized using an ECL chemiluminescence kit (GE Healthcare).

Ub transfer assays of UBC13~Ub

The reaction mixture (25 μl) contained 20 mM HEPES–NaOH (pH 7.5), 50 mM NaCl, 0.2 mg/ml BSA, 1 mM DTT, 5 mM $MgCl_2$, 1 mM ATP, poly(dA)-oligo(dT) (GE Healthcare) (100 ng) as the source of mpssDNA, E1 (1.7 pmol), MMS2–UBC13 complexes (83.7 pmol dimer) and Ub (174 pmol). After incubation at 30°C for 10 min, the reactions were quenched by the addition of *N*-ethylmaleimide (NEM) (5 mM) and EDTA (25 mM) for 1 min (25,26). HLTF (1.3 pmol) was introduced and the mixture was allowed to incubate for an additional 2 min. Reaction products were analyzed by immunoblot.

Purification of ^{His}Ub-charged RAD6A–RAD18

The reaction mixture (5 ml) contained 20 mM HEPES–NaOH (pH 7.5), 5 mM $MgCl_2$, 1 mM ATP, E1 (1.2 nmol), RAD6A–^{His}RAD18 complexes (partially purified fraction, ~3 nmol trimer) and ^{His}Ub (46 nmol). After incubation at 20°C for 10 min, the mixture was immediately applied to a HiTrap Heparin HP column (1 ml) at 4°C. RAD6A–^{His}RAD18 complexes were eluted with a linear gradient of NaCl. Aliquots of peak fractions were frozen in liquid nitrogen and stored at −80°C.

RESULTS

Polyubiquitination of PCNA by *en bloc* Ub chain transfer

To explore the molecular mechanism of PCNA ubiquitination in humans, we developed an *in vitro* ubiquitination reaction system reconstituted with recombinant human proteins (Supplementary Figure S1A) (7,19). As shown in Figure 1A, polyubiquitination of PCNA was readily apparent when MMS2–UBC13 and HLTF-containing reactions were supplemented with RAD6A–RAD18, E1, mpssDNA and replication factor C (RFC), a PCNA loader, all of which are required for PCNA monoubiquitination (7,13). No PCNA ubiquitination was detected when RAD6A–RAD18 or E1 was omitted, or when PCNA was replaced with a mutant derivative carrying a K164R single amino acid substitution; small amounts of ubiquitinated PCNA were observed when mpssDNA or RFC was omitted. When Ub was replaced with an Ub^{K63R} mutant, only monoUb-PCNA was observed, which suggested that the Ub chain linkage was via a Lys63 linkage (Figure 1B) (13).

Analysis of the time course of the reaction indicated that the accumulation of polyubiquitinated products was consistent over time, as opposed to smaller products forming first and then gradually converting into larger products (Figure 1C). This property was consistently observed under other assay conditions with different enzyme concentrations (Supplementary Figure S2). These results suggested that PCNA polyubiquitination may take place via *en bloc* transfer of a Ub chain (27) that is first formed on E2 via a thioester bond at a catalytic cysteine (E2~Ub_n) (Figure 1D), and then transferred to PCNA. To test this hypothesis, the presence of unanchored Ub chains was assessed by immunoblot following treatment with a reducing agent, to hydrolyze the thioester bond of E2~Ub_n (25). Following SDS–polyacrylamide gel electrophoresis (PAGE), immunoblot analysis with an anti-Ub antibody showed the formation of unanchored Ub chains with Lys63 linkages (Figure 1E and F). Efficient formation of Ub multimers was completely dependent on MMS2–UBC13 and E1, but not on RAD6–RAD18, RFC or PCNA. Interestingly, Ub multimer formation required the presence of HLTF and mpssDNA, while a small amount of Ub_2 was formed in their absence, as previously observed when Ub was incubated with MMS2–UBC13 and E1 (15,28). To obtain direct evidence of UBC13~Ub_n formation, reactions were analyzed by SDS–PAGE under non-reducing conditions in order to prevent hydrolysis of the thioester bond, followed by immunoblot analysis with an anti-UBC13 antibody (25). The results clearly demonstrated the formation of UBC13~Ub_n (Figure 1G), which disappeared upon treatment with a reducing agent (Figure 1H). There was only slight accumulation of UBC13 conjugated to long chain Ub (>Ub_5) (Figure 1G), which was in contrast to polyubiquitinated PCNA and unanchored Ub chains, where larger products were relatively abundant (Figure 1A and E; see also 'Discussion' section). The protein components required for efficient UBC13~Ub_n ($n \geq 2$) formation (Figure 1G) were the same as those required for unanchored Ub multimer formation (Figure 1E). Notably, when either HLTF or mpssDNA was omitted, formation of Ub chains and UBC13~Ub_n was severely reduced. Small amounts of Ub_2 and UBC13~Ub_2 were detected, however, and this was dependent on MMS2–UBC13 (Figure 1E and G). These results suggested that mpssDNA is involved in the same biochemical step as HLTF, probably as a co-factor in Ub chain formation.

To test this putative mechanism of *en bloc* Ub chain transfer of preformed chains of UBC13~Ub_n to PCNA, we examined whether pre-incubation of MMS2–UBC13 and HLTF with Ub before the addition of PCNA could accelerate the immediate formation of poly-Ub PCNA with long Ub chains. We set up the following experiments, as shown in Figure 1I. In Ex. 1, RAD6A–RAD18, MMS2–UBC13, E1, Ub, mpssDNA and HLTF were pre-incubated for 5 min, and then combined with a PCNA–preassembly mixture containing PCNA, RFC and mpssDNA. In Ex. 2, RAD6A–RAD18, MMS2–UBC13, E1, Ub and mpssDNA were pre-incubated for 5 min and then combined with a PCNA–preassembly mixture together with HLTF. After a brief period of additional incubation for 15 s, the reaction products were analyzed by immunoblot using an anti-PCNA antibody. In Ex. 1, but not Ex. 2, Ub chains would be assembled on E2 by HTLF prior to the addition of PCNA for *en bloc* Ub chain transfer; by contrast, a step-wise addition of Ub onto PCNA would yield similar kinetics in both experiments. A different size distribution of poly-Ub PCNA was

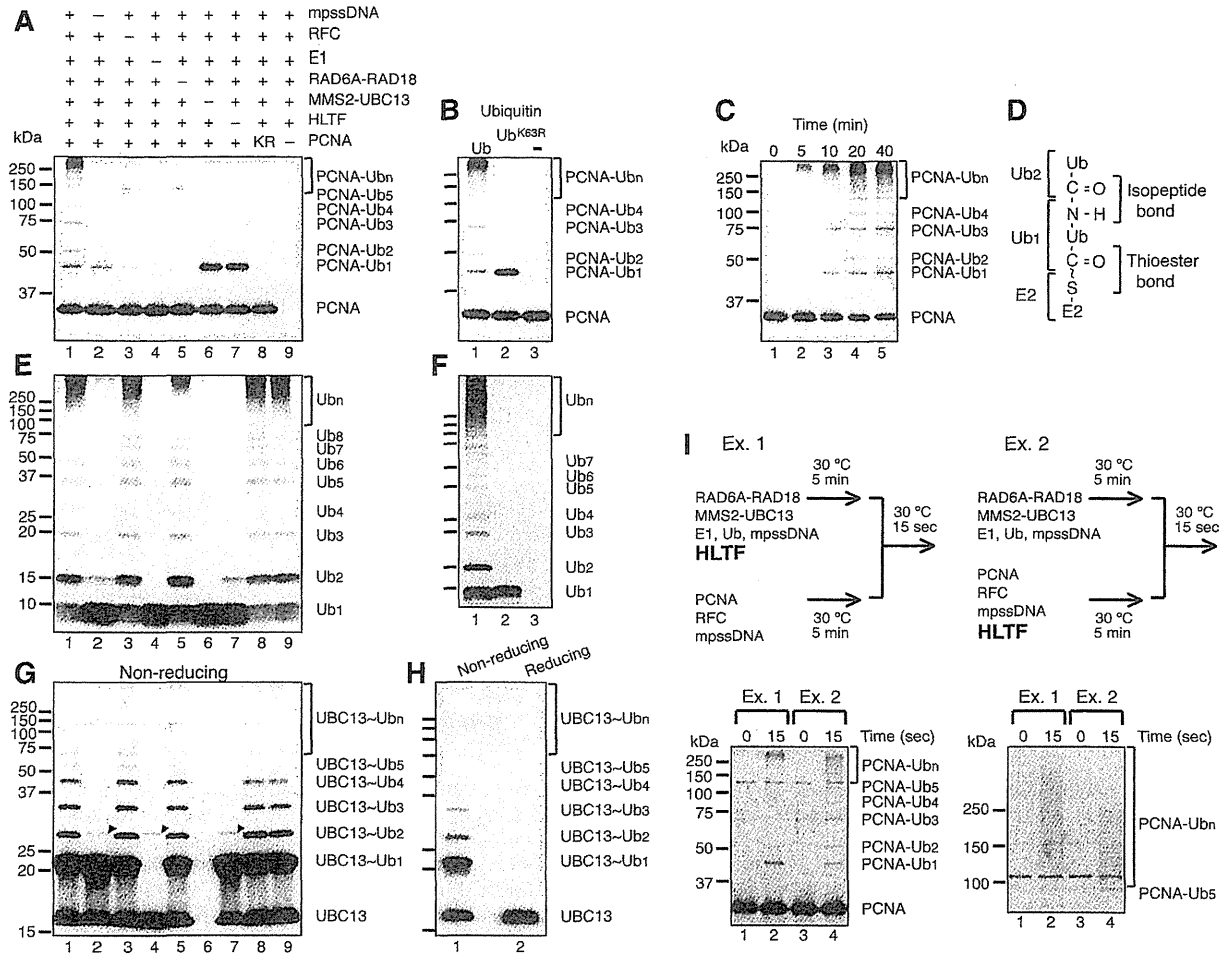

Figure 1. Polyubiquitination of PCNA by *en bloc* Ub chain transfer. (**A**) *In vitro* reconstituted PCNA polyubiquitination reactions. Reactions were reconstituted with PCNA, mpssDNA, RFC, E1, RAD6A–RAD18, MMS2–UBC13, HLTF and Ub. Reaction products were analyzed by immunoblot using an anti-PCNA antibody. –, omitted factor; KR, $PCNA^{K164R}$. (**B**) Lys63-linked Ub chain formation on PCNA was analyzed by immunoblot using an anti-PCNA antibody. (**C**) Time course of polyubiquitination. Reaction products were analyzed by immunoblot using an anti-PCNA antibody. (**D**) Chemical structure of the thiol-linked Ub dimer on E2 ($E2{\sim}Ub_2$). (**E** and **F**) Unanchored Ub chain formation. The products of (A) and (B) were probed with an anti-Ub antibody in (E) and (F), respectively. In these blots, the signals corresponding to ubiquitinated PCNA are not detectable. The amount of PCNA trimer in the reaction was 1 pmol (3 pmol monomer), whereas the amount of ubiquitin was 174 pmol; thus, the estimated signal intensity of total ubiquitinated PCNA was <1% that of ubiquitin. (**G** and **H**) $UBC13{\sim}Ub_n$ formation. The products of (A) untreated by a reducing agent were probed with an anti-UBC13 antibody (G). Presumed dimers of UBC13 linked via S–S bond formation during sample preparation are indicated by arrowheads. The products of lane 1 in (G) treated with or without a reducing agent were analyzed by immunoblot using an anti-UBC13 antibody (H). (**I**) Transfer of pre-formed Ub chains to PCNA. The experimental designs are shown in the upper panel (see text for details). The reaction products were analyzed by electrophoresis under two different conditions and then probed with an anti-PCNA antibody.

observed under the two reaction conditions (Figure 1I and Supplementary Figure S3). In Ex. 1, the accumulation of large products (>150 kDa) was quite prominent. In contrast, in Ex. 2, intermediate sized poly-Ub PCNA (50 to ≤ 150 kDa) was abundant, but large products (>250 kDa) were much less abundant compared to Ex. 1. These results supported *en bloc* Ub chain transfer under these *in vitro* experimental conditions. To obtain further evidence, we analyzed detailed mechanisms underlying the hypothesized *en bloc* Ub chain transfer in additional experiments (see below).

Essential function of HLTF in $UBC13{\sim}Ub_n$ formation

To further investigate the role of HLTF in PCNA polyubiquitination, we analyzed $UBC13{\sim}Ub_n$ formation separately from PCNA polyubiquitination. The minimal set of factors necessary for $UBC13{\sim}Ub_n$ formation (Figure 2A) as well as for unanchored Ub chain formation (Figure 2B) were HLTF, MMS2–UBC13, E1, Ub and mpssDNA. Replacing wild-type Ub with its mutant derivative, Ub^{K63R}, confirmed that the multiple bands observed were Lys63-linked Ub chains on UBC13 (Figure 2C, lane 4). Furthermore, when Ub was replaced with ^{FLAG}Ub, the bands migrated more slowly (Figure 2C, lane 3), which indicated that they contained Ub molecules.

The RING domain of E3 serves an essential function in the ligase reaction by mediating the interaction with E2 (29,30). To determine whether the ligase activity of HLTF was necessary for Ub chain formation, we constructed an HLTF RING mutant in which the conserved cysteine

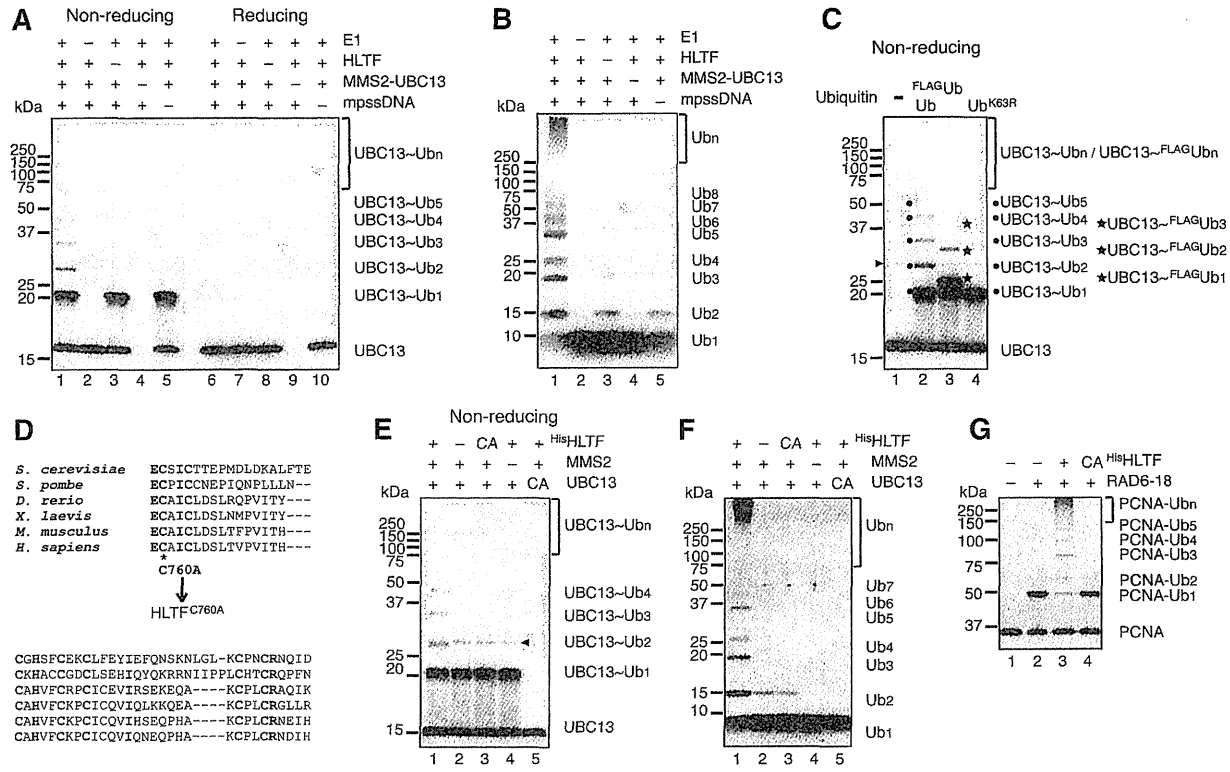

Figure 2. Analysis of UBC13~Ub_n formation. (**A**) Formation of thiol-linked Ub chains on UBC13 with the minimal set of factors. The reactions were reconstituted with mpssDNA, E1, MMS2–UBC13, HLTF and Ub. The reaction products treated with or without a reducing agent were analyzed by immunoblot using an anti-UBC13 antibody. –, omitted factor. (**B**) Formation of Ub chains with the minimal set of factors. The reaction products in (A) were treated with a reducing agent and then analyzed by immunoblot using an anti-Ub antibody. (**C**) Evidence that the multiple thiol-linked bands on UBC13 are Lys63-linked Ub chains. The reaction products untreated by a reducing agent were analyzed by immunoblot using an anti-UBC13 antibody. The positions of UBC13~Ub_n and UBC13~$^{FLAG}Ub_n$ are indicated by dots and stars, respectively. Presumed dimers of UBC13 linked via S–S bond formation during sample preparation are indicated by an arrowhead. (**D**) Multiple sequence alignment of the RING fingers of human HLTF and its orthologs. The conserved cysteine residue (marked with asterisk) was replaced with an alanine. (**E** and **F**) Analysis of HLTF mutants. The reaction products were treated with (F) or without (E) a reducing agent and then analyzed by immunoblot using an anti-UBC13 antibody (E) and an anti-Ub antibody (F). –, omitted factor; CA for ^{His}HLTF, ^{His}HLTF^{C760A}; CA for UBC13, UBC13^{C87A}. Presumed dimers of UBC13 linked via S–S bond formation during sample preparation are indicated by an arrowhead. (**G**) Catalytic activity of HLTF is essential for polyubiquitination of PCNA. PCNA polyubiquitination reactions were performed using ^{His}HLTF or ^{His}HLTF^{C760A} (CA) under standard reaction conditions. The reaction products were analyzed by immunoblot using an anti-PCNA antibody.

residue (C760) of the RING domain was replaced with an alanine (Figure 2D). Histidine-tagged wild-type and mutant HLTF (^{His}HLTF and ^{His}HLTF^{C760A}, respectively) were partially purified (Supplementary Figure S1B) and eluted in the same fraction as untagged HLTF from a gel filtration column, which confirmed the integrity of them to be preserved. ^{His}HLTF was able to support Ub chain formation as efficiently as untagged HLTF, whereas the mutant protein was unable to do so (Figure 2E and F, lanes 3). Thus, Ub chain formation was dependent on the E3 ligase activity of HLTF. Additionally, a mutant form of UBC13 (UBC13^{C87A}) (Supplementary Figure S1B), in which the conserved cysteine residue involved in thioester bond formation with Ub was replaced with alanine, did not support chain formation (Figure 2E and F, lanes 5). Finally, replacing MMS2–UBC13 complexes with UBC13 monomers (Supplementary Figure S1B) demonstrated that MMS2 was also required for Ub chain formation (Figure 2E and F, lanes 4).

Using the HLTF RING mutant, we confirmed that the catalytic activity of HLTF was required for PCNA polyubiquitination, as well as for UBC13~Ub_n formation (Figure 2G). These results were consistent with the idea that HLTF mediates UBC13~Ub_n formation and then the resultant Ub chain is transferred *en bloc* to PCNA.

Analysis of UBC13~Ub_n formation

UBC13-linked polyubiquitin chains could be generated through an aminolysis-based transfer reaction between neighboring UBC13~Ub molecules, in which the ε-amino group of Lys63 of one Ub molecule attacks the thioester-linked carbonyl of the neighboring Ub molecule on UBC13 (25,27) (Figure 3A, schematic). To investigate this as a possible mechanism, UBC13 in complex with MMS2 was first charged with either wild-type Ub or Ub^{K63R} in the presence of E1 and mpssDNA for 10 min. After quenching for 1 min, by the addition of NEM and EDTA, to inactivate uncharged UBC13 and E1 (25,26), the reaction mixture was supplemented with HLTF and then incubated for an additional 2 min. HLTF-dependent Ub chain formation, as evidenced by the appearance of UBC13~Ub_n ($n \geq 3$), was observed with Ub, but not with Ub^{K63R} (Figure 3B), although a significant amount of

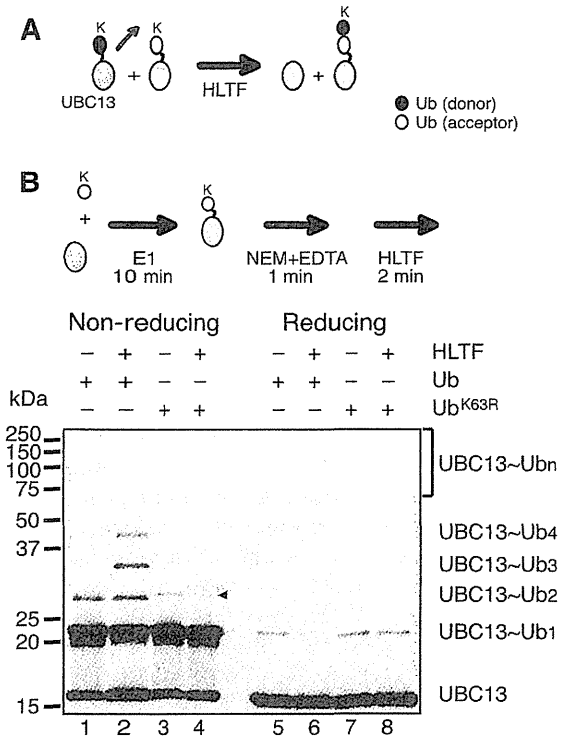

Figure 3. Ub transfer reactions between UBC13~Ub molecules. (**A**) A proposed mechanism of E2~Ub_n formation. A red arrow depicts the direction of Ub movement. MMS2 was included in the reactions by omitted from the schematic. (**B**) Analysis of Ub transfer reactions between UBC13~Ub molecules. The experimental design is shown in the upper panel (see text for details). The reactions were reconstituted with the minimal set of factors (mpssDNA, E1, MMS2–UBC13, HLTF and Ub). The reaction products were treated with or without a reducing agent and then analyzed by immunoblot using an anti-UBC13 antibody. –, omitted factor. Presumed dimers of UBC13 linked via S–S bond formation during sample preparation are indicated by an arrowhead.

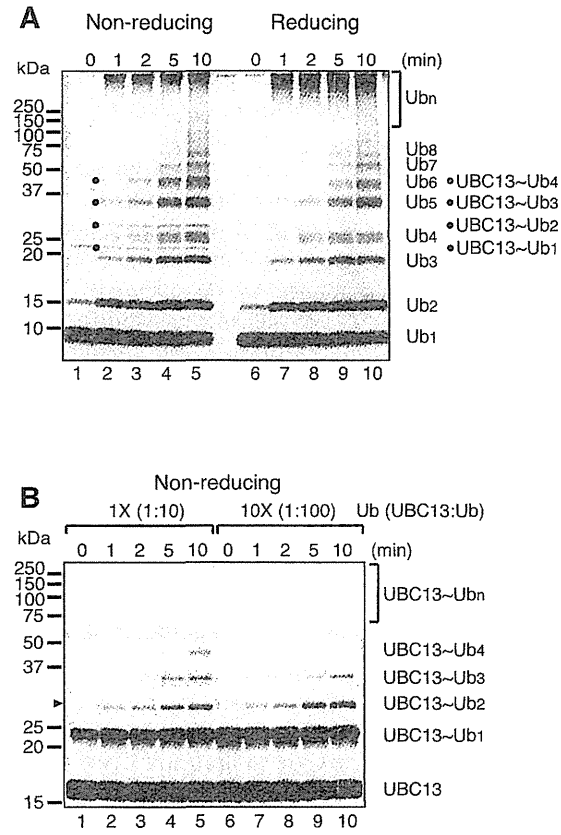

Figure 4. Preferential utilization of UBC13~Ub as Ub acceptor by HLTF. (**A**) Time-course of chain formation using the minimal set of factors. Reaction mixtures containing mpssDNA, E1, MMS2–UBC13 and Ub were pre-incubated for 10 min and then the reactions were started by adding HLTF and incubated for the indicated times. Reaction products were treated with or without a reducing agent and then analyzed by immunoblot using an anti-Ub antibody. (**B**) UBC13~Ub_n competition assays. Reactions in the presence of a 10-fold excess of Ub (10×) were compared to those under standard reaction conditions (1×) with the minimal set of factors. The molecular ratios of UBC13 to Ub are shown in parentheses. Reaction mixtures were pre-incubated without HLTF for 1 min and then the reactions were started by adding HLTF and incubated for the indicated times. Reaction products untreated by a reducing agent were analyzed by immunoblot using an anti-UBC13 antibody. Presumed dimers of UBC13 linked via S–S bond formation during sample preparation are indicated by an arrowhead.

UBC13~Ub_2 was formed in the absence of HLTF under these reaction conditions (Figure 3B, lane 1). The reaction products were sensitive to treatment with a reducing agent, which indicated that they possessed thiol-linked Ub chains (Figure 3B, lanes 5–7). We also confirmed that UBC13~Ub_n formed in these reactions was not a product of recharging due to incomplete quenching (Supplementary Figure S4; see also Supplementary Note for Supplementary Figure S4). Collectively, these results demonstrated that HLTF catalyzes UBC13-Ub_n formation by enhancing an aminolysis-based transfer reaction between two UBC13~Ub molecules.

Preferential utilization of UBC13~Ub as a Ub acceptor by HLTF

Next, we investigated whether the transfer reaction between two UBC13~Ub molecules, as depicted in Figure 3A, was the predominant mechanism, or if Ub moieties from UBC13~Ub were transferred to uncharged Ub as well as a UBC13~Ub. This was addressed by analyzing the time course of the reaction. Reaction mixtures were pre-incubated without HLTF for 10 min, and then reaction products were removed at different time points after the addition of HLTF and analyzed by immunoblot using an anti-Ub antibody (Figure 4A). Comparison of the products formed under non-reducing and reducing conditions demonstrated that UBC13~Ub_n was present only under non-reducing conditions, while unanchored Ub chains were present under both conditions (Figure 4A; quantified in Supplementary Figure S5A). In all of these reactions, Ub was present in ~20-fold molecular excess over UBC13~Ub (see legend for Supplementary Figure S5B). Thus, if Ub was transferred to uncharged Ub as well as UBC13~Ub, the formation of unanchored Ub chains would predominate. However, unanchored and UBC13-linked Ub chains were detected at equivalent levels at the early time points (Figure 4A and Supplementary Figure S5A), which suggested that HLTF preferentially transfers Ub to UBC13~Ub rather than uncharged Ub, and that UBC13~Ub is a preferred Ub acceptor for HLTF (Supplementary Figure S5B).

To confirm the preferential utilization of UBC13~Ub as an Ub acceptor, the experiment was repeated, this time with Ub at 100-fold molar excess over UBC13 (Figure 4B). Under these conditions, excess Ub would strongly compete against UBC13~Ub_n formation. Alternatively, if UBC13~Ub was the preferred substrate, UBC13~Ub_n formation would be unaffected by excess Ub. The time course of the reaction clearly showed only a slight inhibitory effect of 100-fold excess Ub (<2-fold), providing additional evidence of the specificity of HLTF for UBC13~Ub as a Ub acceptor. Additionally, we demonstrated that the formation of unanchored Ub chains was strongly decreased at low concentrations of uncharged Ub (Supplementary Figure S6 and Supplementary Note for Supplementary Figure S6), which indicated that the unanchored Ub chains were by-products generated, at least in part, by Ub (chain) transfer from UBC13~Ub_n ($n \geq 1$) to uncharged Ub (see Supplementary Note for Supplementary Figure S6).

Analysis of the mechanism of polyubiquitination of PCNA

One current theory of polyubiquitination of PCNA holds that the Ub chain forms on the Ub moiety of monoUb-PCNA, and that the role of RAD6A–RAD18 is simply to provide a source of monoUb-PCNA. Based on this model, RAD6A–RAD18 should be dispensable when pre-formed monoUb-PCNA is supplied as the substrate for the polyubiquitination reaction, as was previously shown using yeast proteins (16). To examine the Ub transfer reaction in more detail, partially ^{His}Ub-modified PCNA (PCNA-^{His}Ub) was purified and used as the substrate. In contrast to previous reports using yRAD5, monoUb-PCNA was a surprisingly poor substrate for PCNA polyubiquitination upon incubation with E1, MMS2–UBC13 and HLTF, although trace amounts of polyUb-PCNA were detected (Figure 5A, lane 2 and Figure 5B, lanes 1–5). When RAD6A–RAD18 was added to the reaction mixture, however, polyUb-PCNA was efficiently generated (Figure 5A, lane 5 and Figure 5B, lanes 6–10). It appeared that polyUb-PCNA species were derived from unmodified PCNA rather than from PCNA-^{His}Ub, because the amount of unmodified PCNA was significantly reduced upon prolonged incubation, while that of PCNA-^{His}Ub remained unchanged (Figure 5B, lanes 6–10). The poor capacity of PCNA-^{His}Ub to act as a substrate for polyubiquitination was not due to any intrinsic property of ^{His}Ub, because it was an excellent substrate for polyubiquitination of unmodified PCNA (Supplementary Figure S7). Furthermore, we also tested a PCNA–Ub^{GG} fusion protein, in which Ub was fused to the C-terminus of PCNA via a six amino acid linker, and the two glycine residues in the C-terminus of the Ub moiety were deleted to avoid aberrant charging reactions (Figure 5C). Here, two different ^{His}PCNA–$Ub^{\Delta GG}$ fusion proteins carrying either a K164R mutation in PCNA or a K63R mutation in Ub were examined. Polyubiquitination of ^{His}PCNA–$Ub^{K63R/\Delta GG}$ was much more prominent than with ^{His}PCNA^{K164R}–Ub^{GG} (Figure 4C), which suggested that HLTF does not prefer the Ub moiety of the ^{His}PCNA–Ub^{GG} fusion protein as an acceptor.

The results described above suggested a novel mechanism of polyubiquitination of PCNA, in which mono- and polyubiquitination are coupled to a certain extent. One possibility is that Ub chains are formed directly on Lys164 of PCNA by HLTF and that RAD6–RAD18 is required for a non-catalytic function. To test this hypothesis, we used a RING mutant of RAD18, in which the conserved isoleucine (I50) and arginine (R51) residues were replaced with alanine (Figure 5D); this mutant has been shown to have reduced ligase activity (21). Histidine-tagged wild-type RAD18 and mutant RAD18 (^{His}RAD18 and ^{His}RAD18$^{I50A/R51A}$, respectively) were partially purified in complex with RAD6A (Supplementary Figure S1D). The protein complexes eluted in the same fraction as untagged RAD6A–RAD18 in gel filtration chromatography, which confirmed the integrity of them to be preserved. RAD6A–^{His}RAD18 (wild-type) was able to support mono- and polyubiquitination of PCNA as well as untagged RAD6A–RAD18 (Figure 5E, lanes 1 and 5). By contrast, in the presence of the RAD18 mutant, very little monoUb- or polyUb-PCNA was produced in the presence or absence of HLTF (Figure 5E, lanes 2 and 6). We also examined a mutant form of RAD6A, RAD6A^{C88A}, in which a conserved cysteine residue (C88) involved in the formation of thioester bonds with Ub was replaced with an alanine. Similar to the RAD18 RING mutant, RAD6A^{C88A} did not support chain formation (Figure 5E, lanes 3 and 7). These results indicated that PCNA polyubiquitination depends on the catalytic cysteine of RAD6A and an intact RING finger of RAD18.

We next considered the possibility that Ub chains may first be formed via Lys63 of the thiol-linked Ub moiety on RAD6 by HLTF and then transferred, together with the proximal Ub pre-bound to RAD6, to Lys164 of PCNA by RAD18. In this case, thiol-linked Ub chains on RAD6A might be detected in a manner that is dependent on MMS2–UBC13 and HLTF. The products of the PCNA polyubiquitination reaction shown in Figure 1G were re-analyzed by immunoblot using an anti-RAD6 antibody. The results clearly demonstrated the formation of multiple RAD6A bands that were dependent on MMS2–UBC13, HLTF, mpssDNA and E1, but independent of PCNA and RFC (Figure 5F). These bands were also sensitive to treatment with a reducing agent (Figure 5G). Notably, RAD6A~Ub_n accumulated under conditions in which Ub chain transfer to PCNA was blocked, i.e. when RFC or PCNA was omitted (Figure 5F, lanes 3 and 9), when PCNA was replaced with PCNA^{K164R} (lane 8), or when the RING mutant of RAD18 was used (Figure 5H). These results strongly suggested that RAD6-linked Ub chains are intermediates between UBC13~Ub_n and polyUb-PCNA.

Analysis of RAD6A~Ub_n formation

Because the presence of RAD6A~Ub_n is a novel observation that has not been reported previously, we investigated

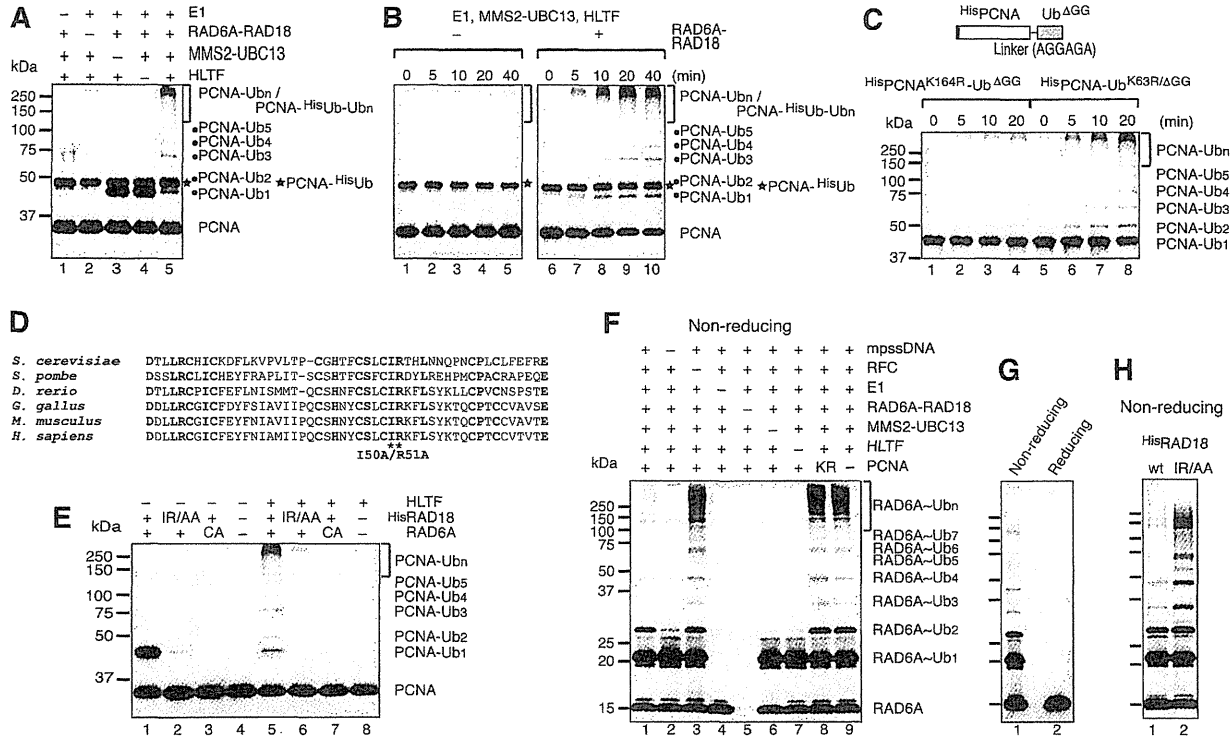

Figure 5. Thiol-linked Ub chains formed on RAD6 are transferred onto PCNA. (**A** and **B**) MonoUb-PCNA is a poor substrate for polyubiquitination. PCNA partially monoubiquitinated with ^{His}Ub was subjected under standard reaction conditions. Reaction products were analyzed by immunoblot using an anti-PCNA antibody. –, omitted factor. (**C**) PCNA ubiquitination assays using ^{His}PCNA–Ub$^{\Delta GG}$ fusion proteins. A schematic of the structure of the fusion protein is shown in the top panel. Reactions were performed with either ^{His}PCNA^{K164R}-Ub$^{\Delta GG}$ or ^{His}PCNA–Ub$^{K63R/\Delta GG}$ instead of PCNA under standard reaction conditions with mpssDNA, RFC, E1, RAD6A–RAD18, MMS2–UBC13, HLTF and Ub, followed by immunoblot using an anti-PCNA antibody. (**D**) Multiple sequence alignment of the RING fingers of human RAD18 and its orthologs. The conserved isoleucine and arginine residues were both replaced with alanines. (**E**) The catalytic activity of RAD6A–RAD18 is required for PCNA polyubiquitination. The reactions were performed using the indicated mutant proteins instead of wild-type protein under standard reaction conditions followed by immunoblot using an anti-PCNA antibody. –, omitted factor; IR/AA, ^{His}RAD18$^{I50A/R51A}$; CA, RAD6A^{C88A}. (**F** and **G**) Ub chain formation on RAD6. The reaction products in Figure 1G and 1H, respectively, were analyzed by immunoblot using an anti-RAD6 antibody. (**H**) Accumulation of RAD6A~Ub$_n$ in complex with the RING mutant of RAD18, RAD18$^{IR/AA}$. The products in lanes 5 and 6 in (E) untreated by a reducing agent were analyzed by immunoblot using an anti-RAD6 antibody (lanes 1 and 2, respectively).

the putative molecular mechanism in more detail. As shown in Figure 6A, RAD6A~Ub$_n$ formation was successfully reconstituted without RFC and PCNA, but was abolished by omission of HLTF, MMS2–UBC13, E1, Ub, mpssDNA or RAD6A–RAD18, which provided additional evidence that these factors are the minimal set of reaction components needed. We confirmed that the multiple bands were Lys63-linked Ub chains on RAD6A by replacing Ub with either ^{FLAG}Ub or Ub^{K63R} (Figure 6B). Furthermore, RAD6A~Ub$_n$ formation was dependent on the catalytic cysteines of UBC13 and RAD6A (Figure 6C, lanes 6 and 7). RAD18 was also an essential component for chain formation (Figure 6C, lane 4), but the RAD18 RING mutant (I50A/R51A) also supported the reaction equally well (Figure 6C, lane 5). Since the RAD18 RING mutant has severely reduced ligase activity in mediating PCNA ubiquitination (Figure 5E) (21), it seems likely that a non-catalytic function of RAD18 other than its ligase activity is required for chain formation on RAD6A. The requirement for the RAD18 subunit might involve a physical interaction between RAD18 and HLTF, as reported previously (11,13). By contrast, the intact RING domain of HLTF was essential for RAD6-Ub$_n$ formation (Figure 6C, lane 3), which indicated that HLTF catalyzes the transfer of Ub molecules from UBC13 to RAD6A.

The formation of RAD6~Ub$_n$ may involve an aminolysis-based transfer reaction between RAD6~Ub and UBC13~Ub$_{n-1}$ (as illustrated in Figure 6D), similar to the mechanism of Ub transfer between UBC13~Ub molecules, as both of the reactions were dependent on the catalytic function of HLTF. In this case, the resulting Ub chain would be expected to be a hybrid between the Ub molecule originally attached to RAD6 and other Ub moieties transferred from UBC13~Ub$_{n-1}$. To investigate the Ub transfer reaction from UBC13~Ub to RAD6~Ub, RAD6A in complex with RAD18 was charged with either ^{His}Ub or ^{His}Ub^{K63R}, and then the modified RAD6A–RAD18 complexes were purified by column chromatography (Figure 6E). The purified complexes supported monoubiquitination of PCNA in the absence of E1 and Ub (Figure 6F), with concomitant reduction in the amount of RAD6A~^{His}Ub and RAD6A~^{His}Ub^{K63R} (Figure 6G). These complexes were then used to test Ub chain formation on RAD6A upon the addition of HLTF and other factors, together with un-tagged Ub^{K63R}, which

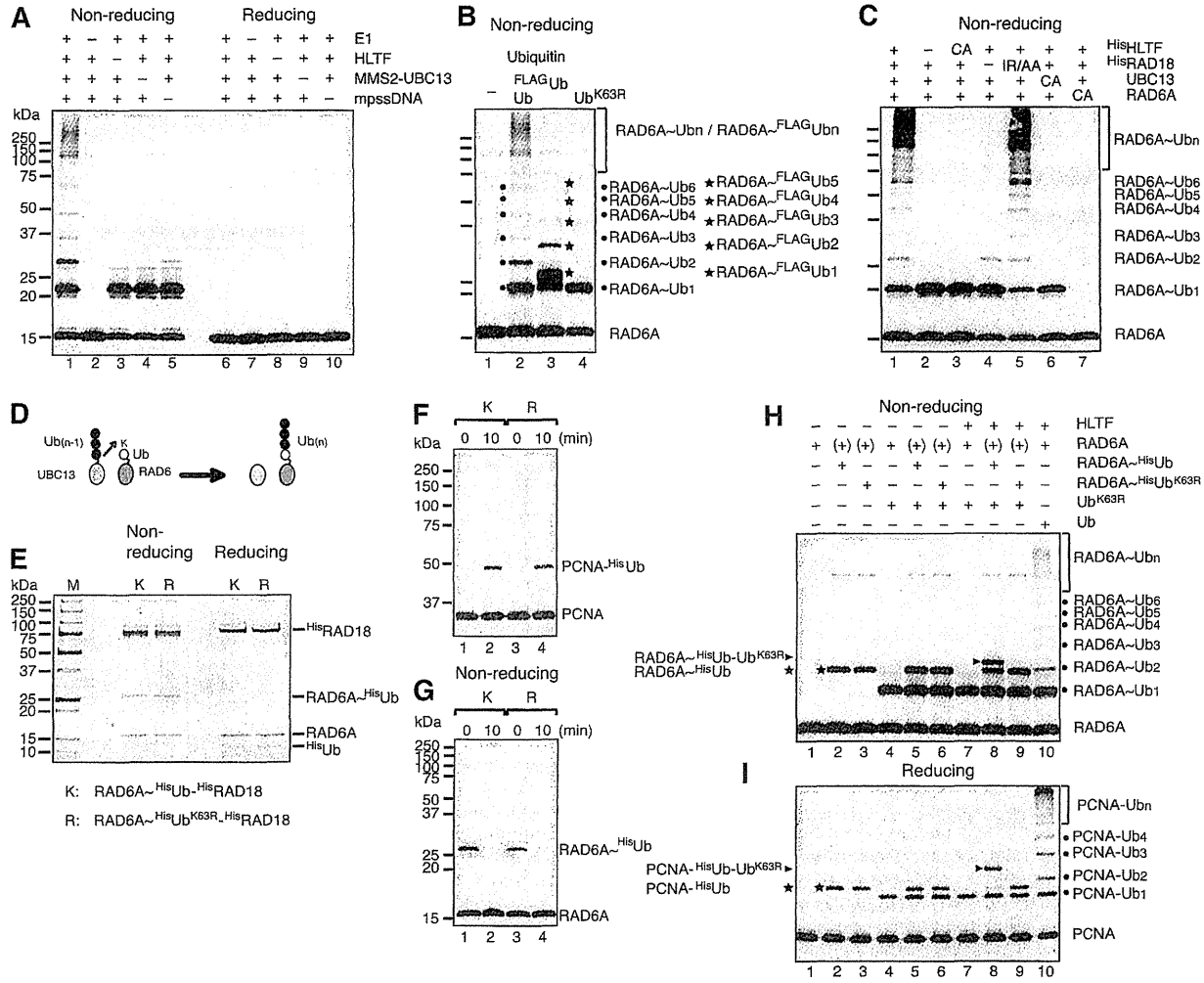

Figure 6. Analysis of RAD6A~Ub_n formation. (**A**) Formation of thiol-linked Ub chains on RAD6A using the minimal set of factors. The reactions were reconstituted with mpssDNA, E1, RAD6A–RAD18, MMS2–UBC13, HLTF and Ub. Reaction products were treated with or without a reducing agent and then analyzed by immunoblot using an anti-RAD6 antibody. –, omitted factor. (**B**) Evidence that the multiple thiol-linked bands on RAD6A are Lys63 linked Ub chains. Reaction products untreated by a reducing agent were analyzed by immunoblot using an anti-RAD6 antibody. The positions of RAD6A~Ub_n and RAD6A~$^{FLAG}Ub_n$ are indicated by dots and stars, respectively. (**C**) Effect of mutants on thiol-linked Ub chain formation on RAD6A. Reaction products untreated by a reducing agent were analyzed by immunoblot using an anti-RAD6 antibody. –, omitted factor; CA for ^{His}HLTF, ^{His}HLTF^{C760A}; IRAA, ^{His}RAD18$^{I50A/R51A}$; CA for UBC13, UBC13^{C87A}; CA for RAD6A and RAD6A^{C88A}. (**D**) Proposed mechanism of RAD6A~Ub_n formation. A red arrow depicts the direction of Ub_n movement. MMS2 and RAD18 were included in the reactions but omitted from the schematic. (**E**) Purified RAD6A~^{His}Ub–^{His}RAD18 and RAD6A~^{His}Ub^{K63R}–^{His}RAD18 complexes treated with or without a reducing agent were analyzed by SDS–PAGE followed by CBB staining. (**F** and **G**) PCNA monoubiquitination reactions were reconstituted with PCNA, mpssDNA, RFC and the indicated complexes (K, RAD6A~^{His}Ub–^{His}RAD18; or R, RAD6A~^{His}Ub^{K63R}–^{His}RAD18) for the indicated times. Reaction products treated with (F) or without (G) a reducing agent were analyzed by immunoblot using an anti-PCNA antibody (F) or an anti-RAD6 antibody (G). (**H**) Analysis of the Ub transfer reaction from UBC13~Ub to RAD6~Ub. Reactions were performed with mpssDNA, E1, MMS2–UBC13, HLTF, Ub^{K63R}, and either RAD6–^{His}RAD18, RAD6A~^{His}Ub–^{His}RAD18, or RAD6A~^{His}Ub^{K63R}–^{His}RAD18 for 2 min. RAD6 molecules shown by (+) were carried from partial charging reactions, as shown in (E). Reaction products untreated with a reducing agent were analyzed by immunoblot using an anti-RAD6 antibody. Lane 10, standard reaction products. (**I**) Analysis of the Ub chain transfer reaction from RAD6~Ub_2 to PCNA. Reactions were performed with PCNA, mpssDNA, RFC, E1, MMS2–UBC13, HLTF, Ub^{K63R}, and either RAD6–^{His}RAD18, RAD6~^{His}Ub–^{His}RAD18, or RAD6~^{His}Ub^{K63R}–^{His}RAD18 for 2 min and then analyzed by immunoblot using an anti-PCNA antibody. Lane 10, standard reaction products.

could be distinguished in size from pre-charged ^{His}Ub. If the expected reactions occurred, Ub^{K63R} would be attached to RAD6~^{His}Ub, but not to RAD6A~^{His}Ub^{K63R}. As shown in Figure 6H, the formation of an additional band was detected in reactions containing RAD6A~^{His}Ub (lane 8), but not RAD6A~^{His}Ub^{K63R} (lane 9), or uncharged RAD6A (lane 7), and the formation was dependent on HLTF (compare lanes 5 and 8). Importantly, this new band migrated between RAD6A~Ub_2 and RAD6A~Ub_3 (see lane 10), which indicated that it was indeed a RAD6A~^{His}Ub–Ub^{K63R} hybrid. Finally, as shown in Figure 6I, the hybrid chain was transferred onto PCNA to generate PCNA-^{His}Ub–Ub^{K63R} (lane 8), which migrated between PCNA-Ub_2 and PCNA-Ub_3 (see lane 10).

The direction of Ub chain elongation in the PCNA polyubiquitination reaction

The results obtained thus far were consistent with a 'seesaw' model of Ub chain elongation (27), which would predict that the direction of chain elongation is PCNA-distal to -proximal, as hypothesized by Hochstrasser (27) (see also 'Discussion' section). We designed a set of experiments to investigate the direction of chain elongation, as depicted schematically in Figure 7A. In Ex. 1, HLTF, RFC, histidine-tagged PCNA (^{His}PCNA) and mpssDNA were pre-incubated for 2 min and then combined with pre-charged UBC13~Ub. The pre-charging reaction was performed for 2 min with E1, MMS2–UBC13 and Ub. After an initial chain elongation reaction for 1 min, the mixture was combined with pre-charged UBC13~^{FLAG}Ub and then incubated for an additional 1 min. The mixture was then combined with pre-charged RAD6A~Ub with RAD18 (pre-charging was performed for 2 min with E1, RAD6A–RAD18 and Ub). After an additional incubation for 1 min, the reaction was terminated by the addition of EDTA for 1 min, and then the catalytic core of Ub-specific protease 2 [^{His}USP2$^{(258-605)}$] (31) was introduced to partially digest the Ub chains. We confirmed that, unlike isopeptidase T, purified ^{His}USP2$^{(258-605)}$ did not react with terminal Ub moieties of K63-linked Ub chains; rather, the ^{His}USP2$^{(258-605)}$ digestion sites on the Ub chain appeared to be at random positions (Supplementary Figure S8). Digestion was performed for 1 min and then terminated by the addition of an equal volume of 8 M urea and 4% Triton X-100. PCNA was immediately purified on Ni-chelating beads and analyzed by immunoblot. The predicted structures of the major products produced by the three different mechanisms of chain elongation are illustrated in Figure 7A. Note that Ub chain elongation reactions were initiated without ^{FLAG}Ub, and the chains were further extended in presence of ^{FLAG}Ub. If chain elongation occurred via a sequential mechanism, Ub and ^{FLAG}Ub would be incorporated onto PCNA at random, because chain elongation would be initiated by the addition of RAD6A–RAD18 in the presence of both UBC13~Ub and UBC13~^{FLAG}Ub. In the case of *en bloc* transfer, there would be differential distribution of Ub and ^{FLAG}Ub within the chain: accumulation of ^{FLAG}Ub at the PCNA-distal end in the case of sequential addition, and accumulation of ^{FLAG}Ub at the PCNA-proximal end in the case of the seesaw mechanism of addition. In experimental scheme Ex. 2 (Figure 7B), the reactions were the same as Ex. 1, except for the order of the addition of UBC13~Ub and UBC13~^{FLAG}Ub. In Ex. 2, pre-charged UBC13~^{FLAG}Ub was incubated first with HLTF, and then pre-charged UBC13~Ub was added. In Ex. 2, sequential chain elongation would result in the incorporation of Ub and ^{FLAG}Ub onto PCNA in a similar fashion as in Ex. 1. In the case of *en bloc* transfer, the pattern of incorporation of Ub and ^{FLAG}Ub would be the opposite of that depicted in Ex. 1. Note that the distribution of each intermediate varies depending on which molecule is the rate-limiting factor for chain elongation. This also means that if the rate-limiting factor in each step of the overall reaction was altered during incubation, the effects would be significant. To avoid this complication, the experiments were completed within 5 min from the first addition of UBC13~Ub to the termination of the reaction, since the velocity of chain elongation was constant for at least 5 min under standard assay conditions.

The products of the reactions outlined in Figure 7A and B were analyzed by immunoblot. Partial digestion of the Ub chains by increasing amounts of ^{His}USP2$^{(258-605)}$ reduced the average sizes of polyUb-PCNA and produced several distinct bands (Figure 7C). Importantly, the band patterns differed between Ex. 1 and 2 (Figure 7C and D), which suggested that the chains were formed predominantly via a seesaw mechanism. This was supported be the following observations:

(1) In both Ex. 1 and 2, the average sizes of polyUb-PCNA were similarly reduced by the addition of ^{His}USP2$^{(258-605)}$ (Figure 7C), which indicated that the Ub chains on PCNA in Ex. 1 and 2 were digested to a similar extent by ^{His}USP2$^{(258-605)}$. When the same samples were analyzed by immunoblot using an anti-FLAG antibody, the patterns differed. In Ex. 1, both the total amount and the average size of the ^{FLAG}Ub-containing chains (detectable by the anti-FLAG antibody) were decreased by the addition of ^{His}USP2$^{(258-605)}$ (Figure 7D), which suggested that a significant fraction of ^{FLAG}Ub had been incorporated into the PCNA-proximal side. By contrast, in Ex. 2, the average size of the ^{FLAG}Ub-containing chains was only slightly decreased, even though signal intensity was clearly reduced (Figure7D). These results indicated that PCNA containing smaller chains as a result of digestion was no longer detectable with the anti-FLAG antibody, suggesting that ^{FLAG}Ub was predominantly incorporated into the PCNA-distal side.

(2) There was substantial accumulation of ^{FLAG}Ub-free bands, indicated by dots, in Ex. 2 (Figure 7C). By contrast, in Ex.1, ^{FLAG}Ub-containing bands were abundant (Figure 7C and D, stars) even after partial digestion, which suggested that a significant fraction of ^{FLAG}Ub was present on the PCNA-proximal side.

These results were consistent with the pattern predicted by a mechanism of *en bloc* transfer of chains formed by the seesaw mechanism of addition (Figure 8B). Collectively, the results of the current study suggest that the seesaw mechanism predominates in PCNA polyubiquitination reactions.

DISCUSSION

Using an *in vitro* ubiquitination reaction system, we were able to obtain detailed information about the mechanism of PCNA polyubiquitination. Although we cannot exclude the possibility that the reaction conditions were

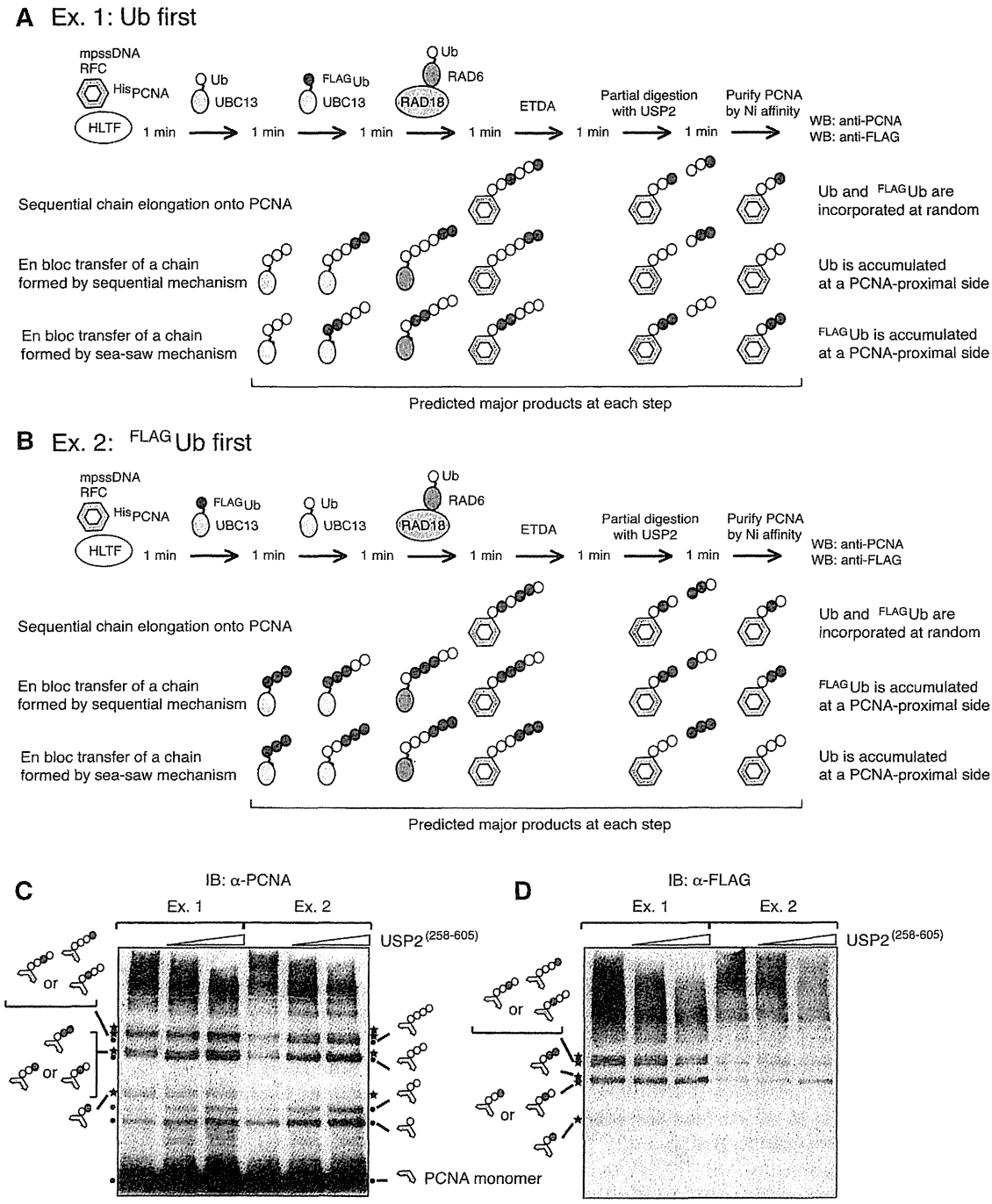

Figure 7. Analysis of the direction of Ub chain elongation. (**A** and **B**) Experimental schemes (see text for details). MMS2 was included in the reactions but omitted from the schematics. (**C** and **D**) Immuonblot analysis using an anti-PCNA antibody to detect total product (C) and an anti-FLAG antibody to detect only ^{FLAG}Ub-containing chains (D). Products containing ^{FLAG}Ub (detected by both the anti-PCNA and anti-FLAG antibodies) are indicated by stars and illustrations. ^{FLAG}Ub-free products (detected by only the anti-PCNA antibody) are indicated by dots and illustrations.

not properly optimized for certain reactions, our results support a novel mechanism of PCNA polyubiquitination that is distinct from, and much more efficient than, the sequential addition reactions of PCNA mono-ubiquitination (Figure 8A) (1,16,17). The mechanism involves pre-formation of a thiol-linked Ub chain on UBC13 and then transfer to RAD6~Ub by HLTF. In this mechanism, HLTF functions as a novel E3 ligase that catalyzes Ub (chain) transfer from UBC13 to the Ub moieties of either UBC13~Ub or RAD6~Ub. This is in contrast to the target protein-specific E3 ligase activity of RAD18, which catalyzes the transfer of Ub chains, as well as Ub monomers, from RAD6 to Lys164 of PCNA. HLTF was also able to catalyze the addition of Ub onto monoUb-PCNA, as described in the sequential addition model, but this activity appeared to be extremely

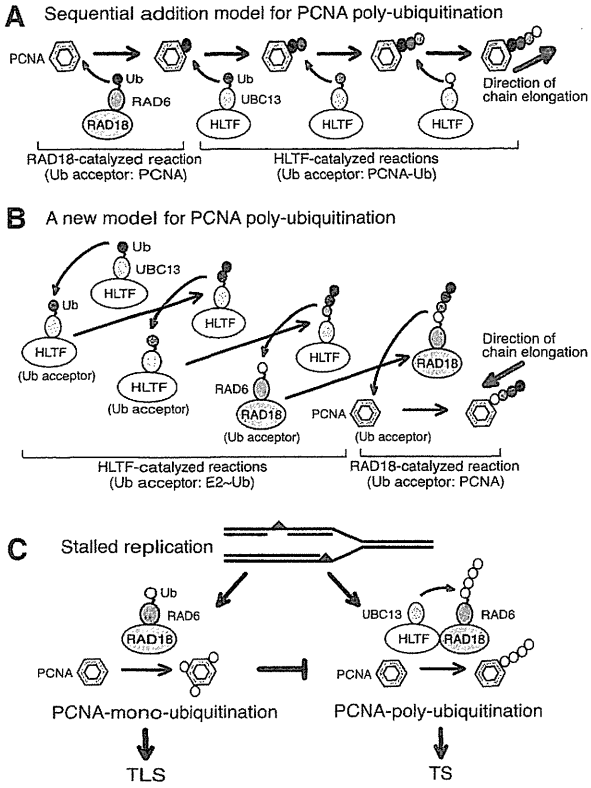

Figure 8. Molecular mechanism of PCNA ubiquitination and implications for the regulation of post-replication repair. MMS2 was omitted to simplify the schematics. A model with MMS2 is shown in Supplementary Figure S9. (**A**) Sequential addition model. RAD18 transfers Ub from RAD6 to PCNA and then HLTF transfers Ub from UBC13 to the terminal Ub moiety of ubiquitinated PCNA. In this model, the Ub chain is elongated in the PCNA-proximal to -distal direction. (**B**) One of potential mechanisms of *en bloc* Ub chain transfer. HLTF transfers Ub from UBC13 to the Ub moiety of UBC13~Ub, generating UBC13~Ub_2. In the next step, the resultant Ub_2 on UBC13 is transferred to the Ub moiety of another UBC13~Ub, generating UBC13~Ub_3. Multiple rounds of this reaction generate long chain UBC13~Ub_n. The Ub chain can be transferred to the Ub moiety of RAD6~Ub, generating RAD6~Ub_{n+1}. RAD18 then transfers the chain from RAD6 to PCNA. In these reactions, the resultant Ub chain has been elongated in the PCNA-distal to -proximal direction. (**C**) Regulation of post-replication repair (see text for details).

low in terms of the substrate specificity of the enzyme (Figure 5A–C). Thus, coupling reactions catalyzed by the two E2–E3 pairs were indispensable for efficient polyubiquitination of PCNA (Figure 5A–C). Our results suggest that HLTF elongates Ub chains via a seesaw type mechanism (27), such that all reactions could be explained by identical biochemical reactions with equivalent substrate specificity. A model is depicted in Figure 8B and Supplementary Figure S9 as one of potential mechanisms of *en bloc* Ub chain transfer. Note that the direction of chain elongation by the seesaw mechanism should be PCNA-distal to -proximal (Figure 8B), which is opposite of that predicted by the conventional model (Figure 8A). This is supported by the data showing that the direction of chain elongation is consistent with a seesaw mechanism of addition (Figure 7).

Our results revealed some interesting properties of HLTF. First, HLTF exhibited a unique specificity for E2~Ub as a substrate. This could represent a biochemical basis for the seesaw mechanism. Second, it functions to regulate Ub chain length. UBC13~Ub_n molecules with long Ub chains ($n \geq 5$) were barely detectable, whereas molecules with short Ub chains ($n \leq 4$) were abundant (Figure 1G). The opposite was observed for RAD6A~Ub_n molecules, with greater accumulation of long chains versus short chains (Figure 5F). These results suggest that the length of the chain attached to UBC13 is enzymatically regulated so that long chains are preferentially transferred to RAD6. Third, DNA was absolutely required for HLTF ligase activity. Since HLTF is a SWI/SNF DNA helicase with a RING domain within the helicase domain, it is likely that the helicase domain is responsible for the interaction with DNA. However, we have been unable to demonstrate a functional interaction between the ligase and helicase domains, as several mutant proteins with alterations in the conserved helicase domain also exhibit ligase activity at levels similar to that of the wild-type protein (Y. Masuda, unpublished data). Previously, it was reported that the Ube2g2 (E2) is capable of producing active site-linked ubiquitin chains with the gp78 (E3), which has been shown to form an oligomer that promotes E2–E2 interactions (32). It is likely that HLTF binding to DNA promotes multimerization of HLTF to stimulate its ligase activity. The precise molecular mechanisms underlying these properties of HLTF remain to be elucidated.

Previously, based on *in vitro* experiments with yRAD5, two groups reported that PCNA polyubiquitination occurs via a conventional, sequential addition reaction mechanism, as depicted in Figure 8A (16,17). The results of these two studies were consistent with some of the genetic studies performed in a *rad18* mutant; namely, that expression of a $PCNA^{K164R}$–Ub fusion protein suppressed defects in both the TLS and TS pathways, but expression of $PCNA^{K164R}$-Ub^{K63R} suppressed only the defect in the TLS pathway, suggesting $PCNA^{K164R}$–Ub, but not $PCNA^{K164R}$–Ub^{K63R}, is polyubiquitinated *in vivo* (33). On the other hand, recent results, also from yeast genetic studies (34,35), demonstrated that expression of $PCNA^{K164R}$–Ub only partially suppresses the *rad18* and *rhp18* mutant phenotype in budding and fission yeast, respectively. In this recent set of studies, $PCNA^{K164R}$–Ub was unable to activate the TS pathway, and this was attributed to the failure to polyubiquitinate the fusion protein. Indeed, $PCNA^{K164R}$–Ub was not polyubiquitinated in either type of yeast (34,35). While these discrepancies in yeast genetic data from different laboratories remain to be resolved, our *in vitro* results are consistent with the more recent genetic data, in that neither $PCNA^{K164R}$–Ub nor monoUb-PCNA was a primary target for polyubiquitination (Figure 5A–C). To directly probe the yRAD5 reaction mechanism, histidine-tagged yRAD5 (^{His}yRAD5) was overexpressed in *E. coli* and partially purified, and then used in our assay system instead of HLTF (Supplementary Figure S6). We expected yRAD5 to interact with the human proteins since HLTF is able to complement the UV sensitivity of a *rad5Δ* strain (13). Indeed, polyubiquitinated PCNA was detected in reactions using partially purified

^{His}yRAD5 (Supplementary Figure S6A). Analysis of the time course of the reaction showed that all of the reaction products, including intermediates, accumulated over time (Supplementary Figure S6B), similar to what was seen with low concentrations of HLTF (Supplementary Figure S2D). Furthermore, monoubiquitinated PCNA was a poor substrate for yRAD5 (Supplementary Figure S6C), similar to that observed for HLTF (Figure 5A). These results suggested that PCNA polyubiquitination by yRAD5 occurs predominantly by *en bloc* transfer of an Ub chain. In the previously reported *in vitro* studies with yRad5, the experiments were for the most part carried out in the absence of RAD6–RAD18, using monoUb-PCNA and either PCNA–Ub fusion proteins (16) or chemically Ub-modified PCNA (17). Even in the presence of RAD6–RAD18, mono- and polyubiquitination were relatively inefficient due to the low activity of RAD6–RAD18 for monoubiquitination (16). Notably, in these studies, the experimental system was designed to detect Ub transfer to monoUb-PCNA. Under similarly uncoupled reaction conditions (i.e. in the absence of RAD6A–RAD18), we were also able to detect Ub transfer to monoUb-PCNA (Figure 5A, lane 2; 5B, lanes 1–5; and 5C, lanes 1–4). The discrepancies between the previous *in vitro* yRad5 studies and the present study are mostly likely due to differences in such reaction conditions. Importantly, however, although the reaction mechanism we defined is completely different from the conventional model, it is essentially consistent with the genetic data; namely both mono- and polyubiquitination are abrogated by inactivation or deletion of either yRAD6 or yRAD18, whereas in the presence of dysfunctional yMMS2, yUBC13, or yRAD5, only polyubiquitination is abrogated (1,2).

If the reaction mechanism we observed *in vitro* mimics what occurs *in vivo*, monoubiquitination and polyubiquitination of PCNA at stalled replication ends would necessarily be promoted separately (Figure 8C). It should be noted that Ub chain formation by UBC13–MMS2 and HLTF required mpssDNA, which differs from the requirement of RAD6–RAD18 for RFC-mediated loading of PCNA on mpssDNA (6,7,36). We hypothesize that PCNA polyubiquitination and activation of the TS pathway is promoted under conditions in which RAD18 and HLTF are coordinately recruited to stalled replication ends, wherein DNA is needed to hold PCNA at the primer terminus (7) and to stimulate HLTF activity. Alternatively, if all three subunits of PCNA at a stalled end are first monoubiquitinated, polyubiquitination cannot occur and the TLS pathway is activated. We have observed that all three subunits of PCNA are efficiently monoubiquitinated at stalled primer ends *in vitro* (7). This scenario could explain how either the TLS or TS pathway is selectively activated at stalled replication sites. The TS pathway would be activated only when a daughter strand that was replicated from the non-damaged parental strand is available and prohibited when such a daughter strand is unavailable. This model is consistent with recent observations from our laboratory that RAD6–RAD18 forms a ternary complex of RAD6A–$(RAD18)_2$ rather than (RAD6A–$RAD18)_2$ and that stable association between RAD6A and RAD18 is an essential requirement for ligase activity (21). These properties of the RAD6–RAD18 complex appear suited for the tight regulation of polyubiquitination of PCNA. If the complex contained two RAD6 molecules, one would have to invoke yet another mechanism involving processive formation of Ub chains on both subunits. Furthermore, if the interaction of RAD6 was dynamic, exchange reactions between RAD6~Ub_n and RAD6~Ub would occur in solution before transfer of the chain to PCNA. The tight regulation of polyubiquitination ensures the timely and appropriate activation of the TS pathway, thereby avoiding irregular recombination. In this manner, eukaryotic cells ensure accurate chromosomal duplication and avoid genetic aberrations that can lead to carcinogenesis.

Finally, we should mention that the seesaw mechanism of ubiquitin chain transfer is similar to the peptidyl transfer reaction of protein synthesis. Conceivably, the concept might be applicable to other E2 and E3 enzymes and another bio-macromolecule synthesis such as oligosaccharides, and may represent a common strategy for the generation of bio-macro-polymers.

SUPPLEMENTARY DATA

Supplementary Data are available at NAR Online: Supplementary Figures 1–10 and Supplementary Notes.

ACKNOWLEDGEMENTS

The authors thank Dr. Toshiki Tsurimoto (Kyushu University, Fukuoka, Japan) for a PCNA-expression plasmid. The authors would also like to express our appreciation to Drs Mark Hochstrasser (Yale University, USA), Haruo Ohmori (Kyoto University, Kyoto, Japan), Richard D. Wood (University of Texas, USA) and Roger Woodgate (NIH, USA) for their comments and suggestions on the manuscript. The authors are furthermore grateful to Yumiko Shintani for making mutants, and Mayumi Hojo, Fumie Okubo, Kazumi Shimamoto, Reiko Tashiro and Mai Yoshida for their laboratory assistance.

FUNDING

Grants-in-Aid from the Ministry of Education, Culture, Sports, Science and Technology of Japan (to Y.M., H.K., H.H., C.M. T.H. and K.K.); Health and Labour Science Research Grants of Japan (to K.K.); the Mitsubishi Foundation and Takeda Science Foundation (to C.M.). Funding for open access charge: JSPS KAKENHI [24310040 to Y.M.].

Conflict of interest statement. None declared.

REFERENCES

1. Friedberg,E.C., Walker,G.C., Siede,W., Wood,R.D., Schultz,R.A. and Ellenberger,T. (2006) *DNA Repair and Mutagenesis*, 2 edn. ASM, Washington, DC.

2. Hoege,C., Pfander,B., Moldovan,G.L., Pyrowolakis,G. and Jentsch,S. (2002) RAD6-dependent DNA repair is linked to modification of PCNA by ubiquitin and SUMO. *Nature*, **419**, 135–141.
3. Kannouche,P.L., Wing,J. and Lehmann,A.R. (2004) Interaction of human DNA polymerase η with monoubiquitinated PCNA: a possible mechanism for the polymerase switch in response to DNA damage. *Mol. Cell*, **14**, 491–500.
4. Watanabe,K., Tateishi,S., Kawasuji,M., Tsurimoto,T., Inoue,H. and Yamaizumi,M. (2004) Rad18 guides polη to replication stalling sites through physical interaction and PCNA monoubiquitination. *EMBO J.*, **23**, 3886–3896.
5. Bienko,M., Green,C.M., Crosetto,N., Rudolf,F., Zapart,G., Coull,B., Kannouche,P., Wider,G., Peter,M., Lehmann,A.R. *et al.* (2005) Ubiquitin-binding domains in Y-family polymerases regulate translesion synthesis. *Science*, **310**, 1821–1824.
6. Garg,P. and Burgers,P.M. (2005) Ubiquitinated proliferating cell nuclear antigen activates translesion DNA polymerases η and REV1. *Proc. Natl Acad. Sci. USA*, **102**, 18361–18366.
7. Masuda,Y., Piao,J. and Kamiya,K. (2010) DNA replication-coupled PCNA mono-ubiquitination and polymerase switching in a human *in vitro* system. *J. Mol. Biol.*, **396**, 487–500.
8. Wood,A., Garg,P. and Burgers,P.M. (2007) A ubiquitin-binding motif in the translesion DNA polymerase Rev1 mediates its essential functional interaction with ubiquitinated proliferating cell nuclear antigen in response to DNA damage. *J. Biol. Chem.*, **282**, 20256–20263.
9. Zhuang,Z., Johnson,R.E., Haracska,L., Prakash,L., Prakash,S. and Benkovic,S.J. (2008) Regulation of polymerase exchange between Polη and Polδ by monoubiquitination of PCNA and the movement of DNA polymerase holoenzyme. *Proc. Natl Acad. Sci. USA*, **105**, 5361–5366.
10. MacKay,C., Toth,R. and Rouse,J. (2009) Biochemical characterisation of the SWI/SNF family member HLTF. *Biochem. Biophys. Res. Commun.*, **390**, 187–191.
11. Motegi,A., Liaw,H.J., Lee,K.Y., Roest,H.P., Maas,A., Wu,X., Moinova,H., Markowitz,S.D., Ding,H., Hoeijmakers,J.H. *et al.* (2008) Polyubiquitination of proliferating cell nuclear antigen by HLTF and SHPRH prevents genomic instability from stalled replication forks. *Proc. Natl Acad. Sci. USA*, **105**, 12411–12416.
12. Motegi,A., Sood,R., Moinova,H., Markowitz,S.D., Liu,P.P. and Myung,K. (2006) Human SHPRH suppresses genomic instability through proliferating cell nuclear antigen polyubiquitination. *J. Cell. Biol.*, **175**, 703–708.
13. Unk,I., Hajdu,I., Fatyol,K., Hurwitz,J., Yoon,J.H., Prakash,L., Prakash,S. and Haracska,L. (2008) Human HLTF functions as a ubiquitin ligase for proliferating cell nuclear antigen polyubiquitination. *Proc. Natl Acad. Sci. USA*, **105**, 3768–3773.
14. Unk,I., Hajdu,I., Fatyol,K., Szakal,B., Blastyak,A., Bermudez,V., Hurwitz,J., Prakash,L., Prakash,S. and Haracska,L. (2006) Human SHPRH is a ubiquitin ligase for Mms2-Ubc13-dependent polyubiquitylation of proliferating cell nuclear antigen. *Proc. Natl Acad. Sci. USA*, **103**, 18107–18112.
15. Hofmann,R.M. and Pickart,C.M. (1999) Noncanonical MMS2-encoded ubiquitin-conjugating enzyme functions in assembly of novel polyubiquitin chains for DNA repair. *Cell*, **96**, 645–653.
16. Parker,J.L. and Ulrich,H.D. (2009) Mechanistic analysis of PCNA poly-ubiquitylation by the ubiquitin protein ligases Rad18 and Rad5. *EMBO J.*, **28**, 3657–3666.
17. Carlile,C.M., Pickart,C.M., Matunis,M.J. and Cohen,R.E. (2009) Synthesis of free and proliferating cell nuclear antigen-bound polyubiquitin chains by the RING E3 ubiquitin ligase Rad5. *J. Biol. Chem.*, **284**, 29326–29334.
18. Fukuda,K., Morioka,H., Imajou,S., Ikeda,S., Ohtsuka,E. and Tsurimoto,T. (1995) Structure-function relationship of the eukaryotic DNA replication factor, proliferating cell nuclear antigen. *J. Biol. Chem.*, **270**, 22527–22534.
19. Masuda,Y., Suzuki,M., Piao,J., Gu,Y., Tsurimoto,T. and Kamiya,K. (2007) Dynamics of human replication factors in the elongation phase of DNA replication. *Nucleic Acids Res.*, **35**, 6904–6916.
20. Tomida,J., Masuda,Y., Hiroaki,H., Ishikawa,T., Song,I., Tsurimoto,T., Tateishi,S., Shiomi,T., Kamei,Y., Kim,J. *et al.* (2008) DNA damage-induced ubiquitylation of RFC2 subunit of replication factor C complex. *J. Biol. Chem.*, **283**, 9071–9079.
21. Masuda,Y., Suzuki,M., Kawai,H., Suzuki,F. and Kamiya,K. (2012) Asymmetric nature of two subunits of RAD18, a RING-type ubiquitin ligase E3, in the human RAD6A-RAD18 ternary complex. *Nucleic Acids Res.*, **40**, 1065–1076.
22. Gu,Y., Masuda,Y. and Kamiya,K. (2008) Biochemical analysis of human PIF1 helicase and functions of its N-terminal domain. *Nucleic Acids Res.*, **36**, 6295–6308.
23. Ecker,D.J., Butt,T.R., Marsh,J., Sternberg,E.J., Margolis,N., Monia,B.P., Jonnalagadda,S., Khan,M.I., Weber,P.L., Mueller,L. *et al.* (1987) Gene synthesis, expression, structures, and functional activities of site-specific mutants of ubiquitin. *J. Biol. Chem.*, **262**, 14213–14221.
24. Haas,A.L. and Rose,I.A. (1982) The mechanism of ubiquitin activating enzyme. A kinetic and equilibrium analysis. *J. Biol. Chem.*, **257**, 10329–10337.
25. Li,W., Tu,D., Brunger,A.T. and Ye,Y. (2007) A ubiquitin ligase transfers preformed polyubiquitin chains from a conjugating enzyme to a substrate. *Nature*, **446**, 333–337.
26. Petroski,M.D. and Deshaies,R.J. (2005) Mechanism of lysine 48-linked ubiquitin-chain synthesis by the cullin-RING ubiquitin-ligase complex SCF-Cdc34. *Cell*, **123**, 1107–1120.
27. Hochstrasser,M. (2006) Lingering mysteries of ubiquitin-chain assembly. *Cell*, **124**, 27–34.
28. Eddins,M.J., Carlile,C.M., Gomez,K.M., Pickart,C.M. and Wolberger,C. (2006) Mms2-Ubc13 covalently bound to ubiquitin reveals the structural basis of linkage-specific polyubiquitin chain formation. *Nat. Struct. Mol. Biol.*, **13**, 915–920.
29. Deshaies,R.J. and Joazeiro,C.A. (2009) RING domain E3 ubiquitin ligases. *Annu. Rev. Biochem.*, **78**, 399–434.
30. Zheng,N., Wang,P., Jeffrey,P.D. and Pavletich,N.P. (2000) Structure of a c-Cbl-UbcH7 complex: RING domain function in ubiquitin-protein ligases. *Cell*, **102**, 533–539.
31. Renatus,M., Parrado,S.G., D'Arcy,A., Eidhoff,U., Gerhartz,B., Hassiepen,U., Pierrat,B., Riedl,R., Vinzenz,D., Worpenberg,S. *et al.* (2006) Structural basis of ubiquitin recognition by the deubiquitinating protease USP2. *Structure*, **14**, 1293–1302.
32. Li,W., Tu,D., Li,L., Wollert,T., Ghirlando,R., Brunger,A.T. and Ye,Y. (2009) Mechanistic insights into active site-associated polyubiquitination by the ubiquitin-conjugating enzyme Ube2g2. *Proc. Natl Acad. Sci. USA*, **106**, 3722–3727.
33. Zhao,S. and Ulrich,H.D. (2010) Distinct consequences of posttranslational modification by linear versus K63-linked polyubiquitin chains. *Proc. Natl Acad. Sci. USA*, **107**, 7704–7709.
34. Pastushok,L., Hanna,M. and Xiao,W. (2010) Constitutive fusion of ubiquitin to PCNA provides DNA damage tolerance independent of translesion polymerase activities. *Nucleic Acids Res.*, **38**, 5047–5058.
35. Ramasubramanyan,S., Coulon,S., Fuchs,R.P., Lehmann,A.R. and Green,C.M. (2010) Ubiquitin-PCNA fusion as a mimic for mono-ubiquitinated PCNA in *Schizosaccharomyces pombe*. *DNA Repair*, **9**, 777–784.
36. Haracska,L., Unk,I., Prakash,L. and Prakash,S. (2006) Ubiquitylation of yeast proliferating cell nuclear antigen and its implications for translesion DNA synthesis. *Proc. Natl Acad. Sci. USA*, **103**, 6477–6482.